Transiting exoplanets

Eamonn Kerins
Jodrell Bank Centre for Astrophysics
University of Manchester

Transiting exoplanets

- Basic theory
- Planet parameters
- Host parameters
- Difficulties (noise, false positives)
- Synergy with radial velocity surveys
- Transiting planet demography
- Exomoon detection

Transits

An intuitive detection method

NASA Stereo B view of a lunar eclipse

Transit geometry

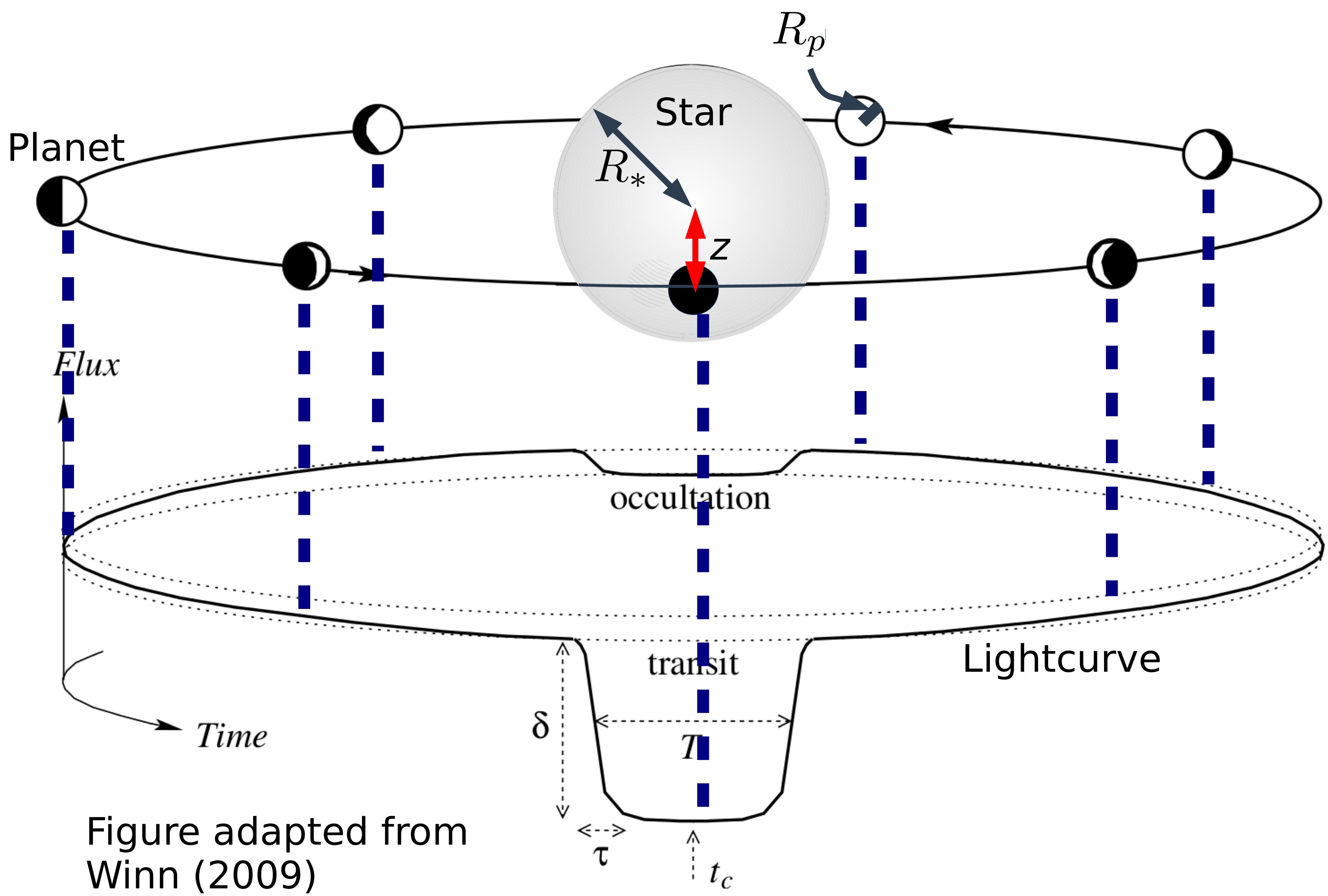

Figure adapted from
Winn (2009)

Transit probability

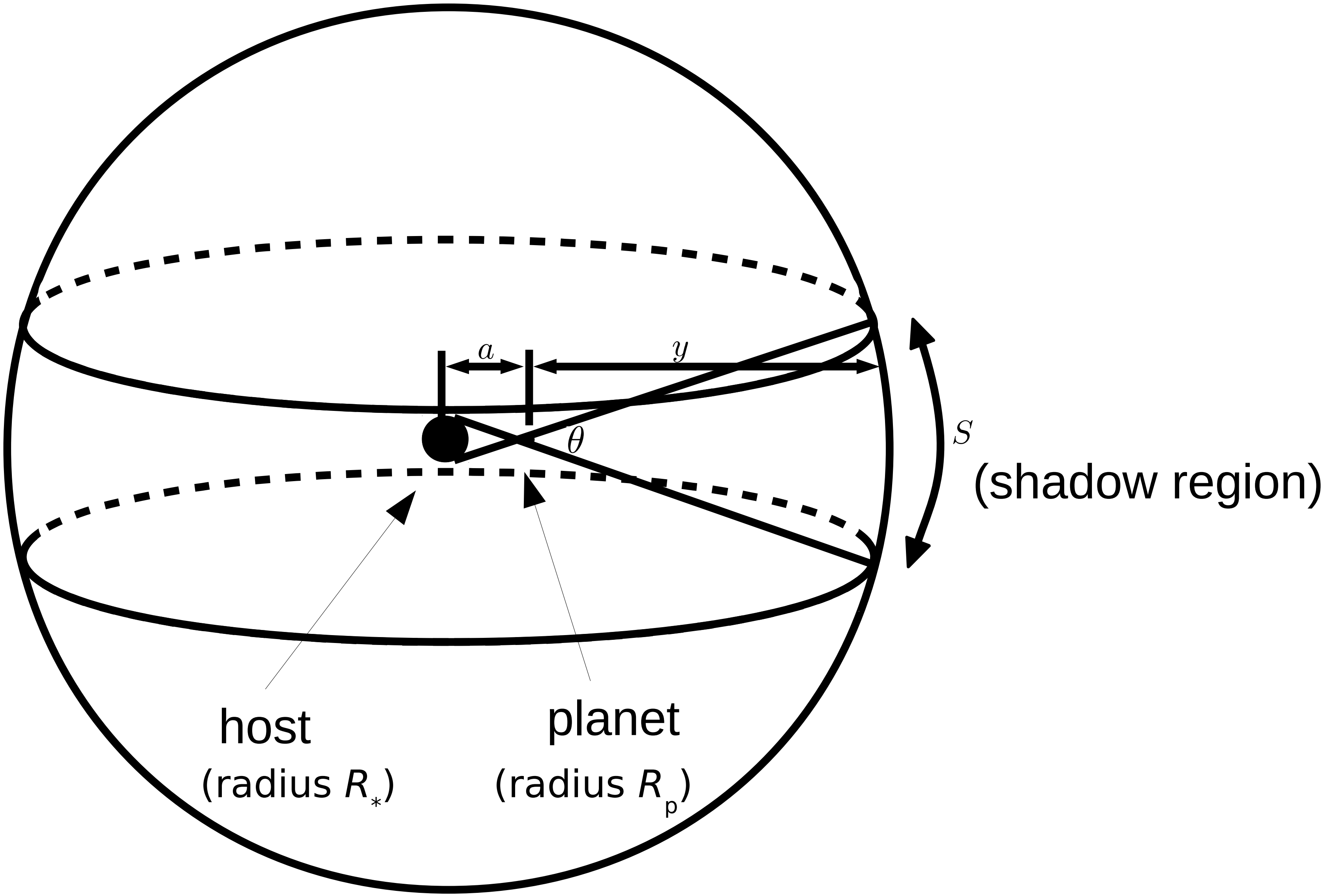

Consider the fraction of the planet's sky swept by its shadow as it orbits its host

Transit probability

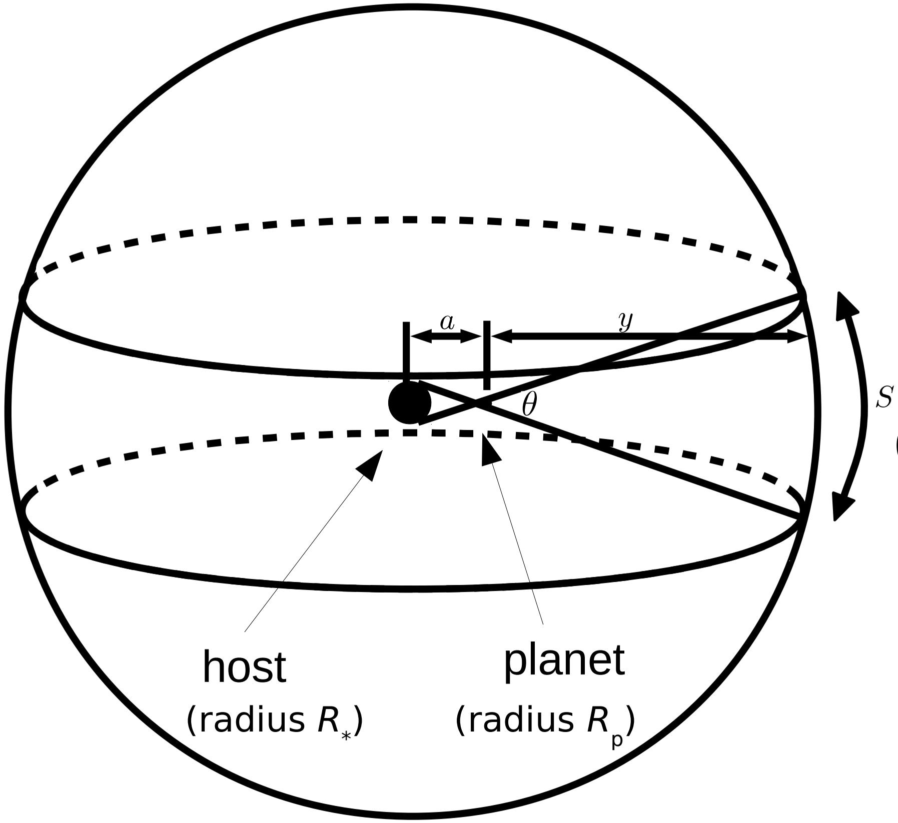

Transit probability is P, where

$$P = \frac{2\pi(a+y)S}{4\pi(a+y)^2} = \frac{S}{2(a+y)}$$

But

$$S = y\theta,\ 2R_* = a\theta \implies S = 2R_* y/a$$

so

$$P = \frac{R_*}{a}\left(\frac{y}{a+y}\right) \simeq \frac{R_*}{a} \qquad (y \gg a)$$

Allowing for finite planet size:

$$P \simeq \frac{R_* + R_p}{a}$$

Transit probability

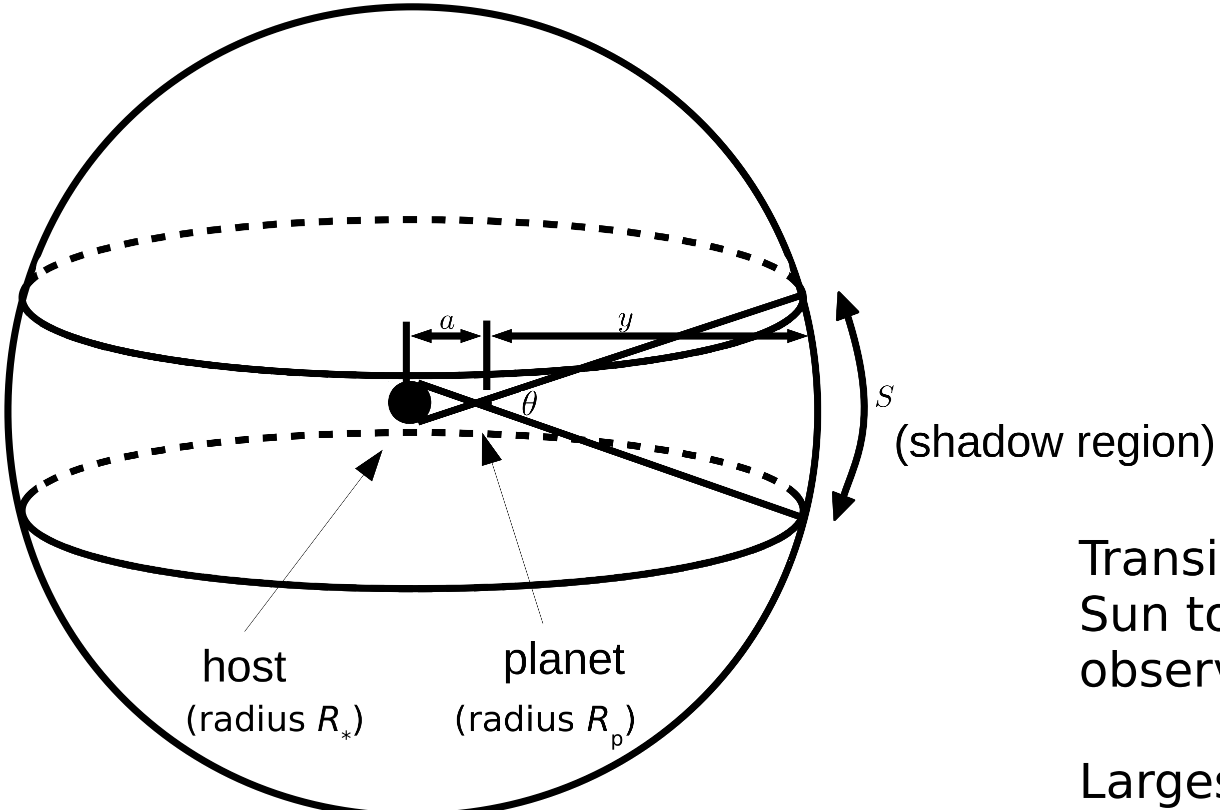

Transit probability for Earth around Sun to a randomly located celestial observer is 0.5%

Largest probability is for Jupiter (~1%), despite being 5 times further from Sun.

⇒ technique is biased towards close in and large planets (hot Jupiters)

Transit depth

For a planet with host separation a and orbit inclination i, producing a sky-projected closest approach distance $z = a \cos i$ between the planet and host, the requirement to observe any transit is that

$$z = a \cos i < R_* + R_p \qquad (1)$$

Minimum flux determined by the maximum fraction of the host's area covered by the planet:

$$F_{\min} = F_*[1 - (R_p/R_*)^2] \qquad (2)$$

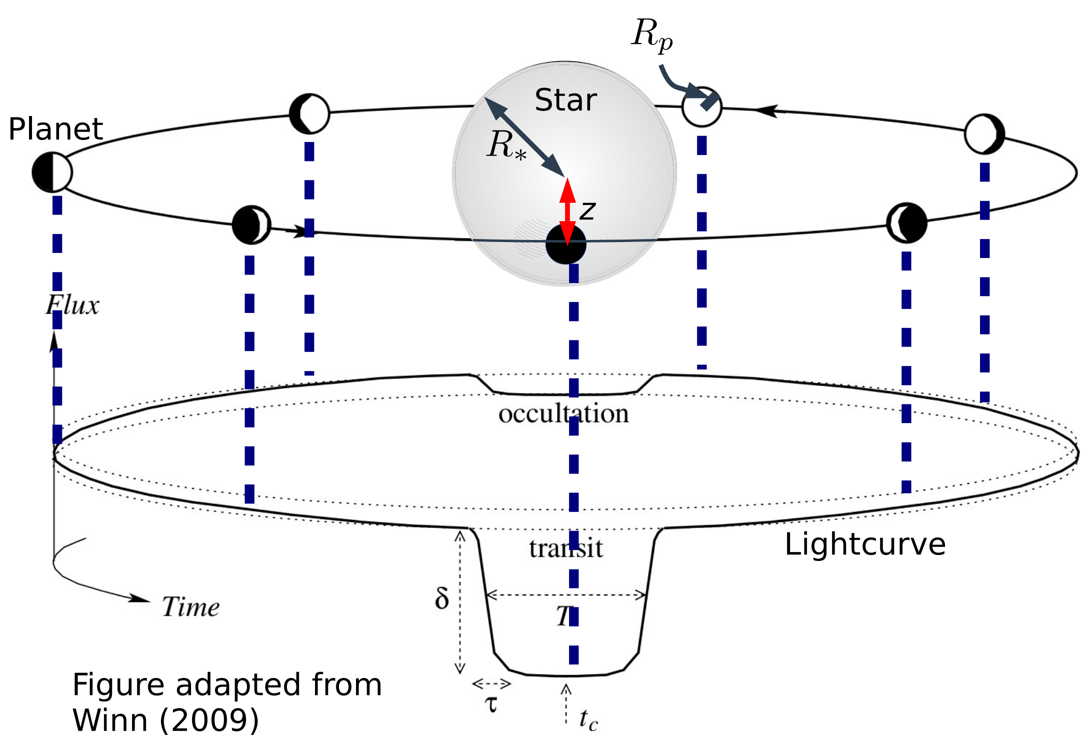

Figure adapted from Winn (2009)

Transit depth

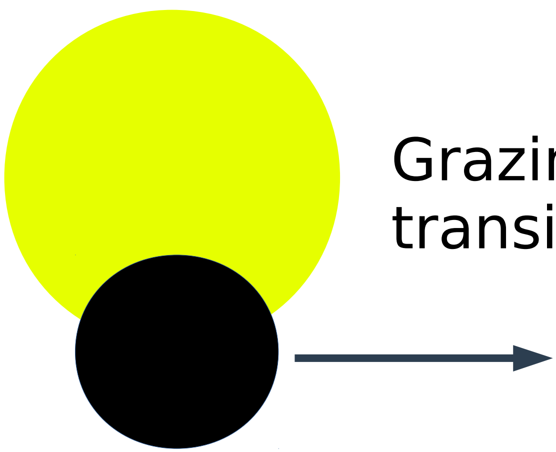

Grazing
transit

Full
transit

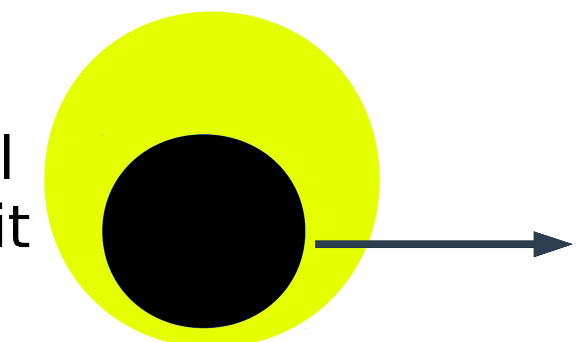

Observed depth also depends on
inclination angle of the planet orbit.

Ingress and egress

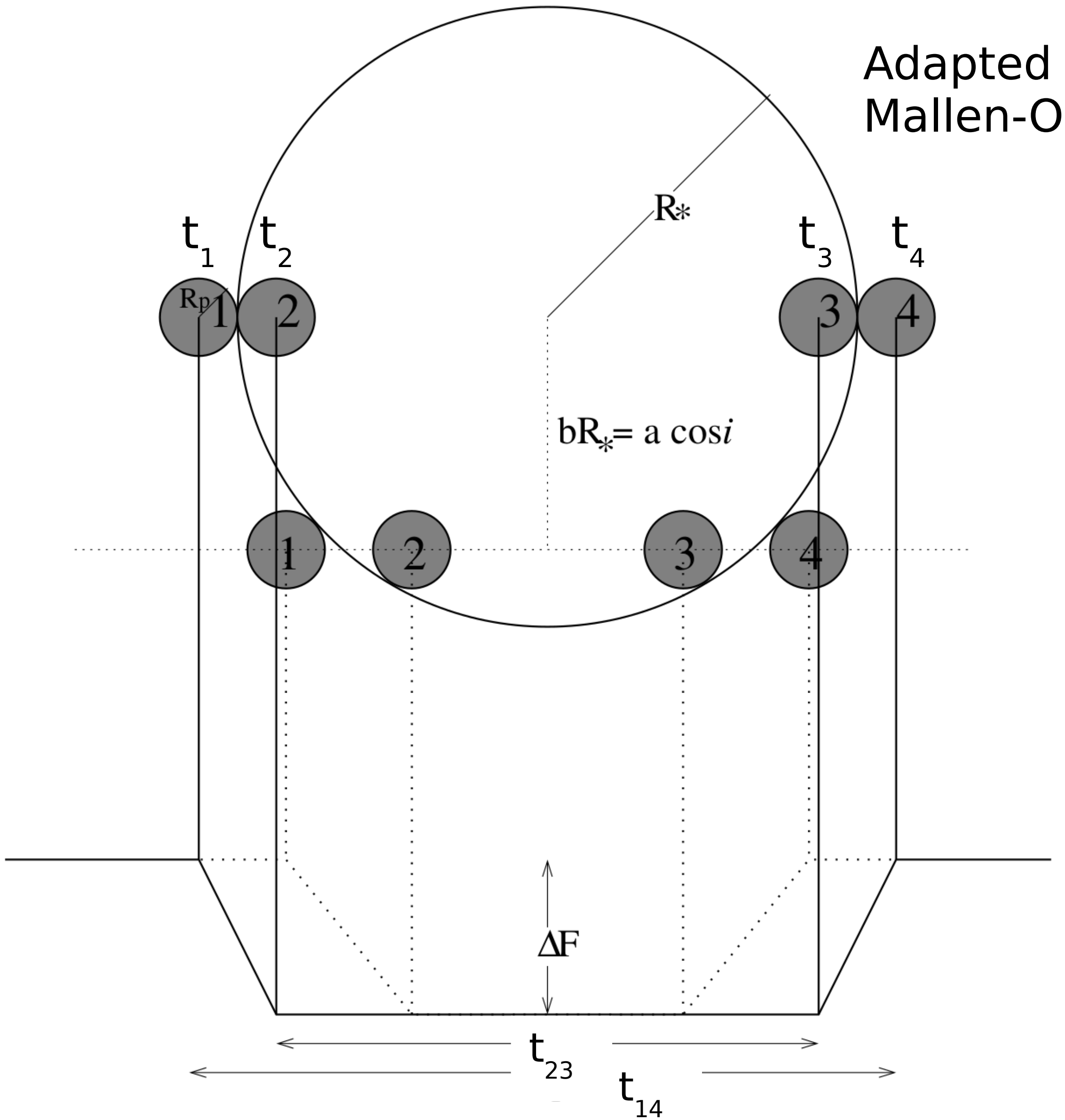

Adapted from Seager & Mallen-Ornelas (2003)

Transit lightcurve

Mandel & Agol (2002) state without proof the analytic formula for a transit lightcurve due to a planet passing in front of a uniform source (no limb darkening):

$$1 - F_*(p, z) = \begin{cases} 0, & 1 + p < z, \\ \dfrac{1}{\pi}\left[p^2\kappa_0 + \kappa_1 - \sqrt{\dfrac{4z^2 - (1 + z^2 - p^2)^2}{4}}\right], & |1 - p| < z \leq 1 + p, \\ p^2, & z \leq 1 - p, \\ 1, & z \leq p - 1, \end{cases}$$

$$\kappa_0 = \cos^{-1}[(p^2 + z^2 - 1)/2pz], \quad \kappa_1 = \cos^{-1}[(1 - p^2 + z^2)/2z]$$

Let’s prove it!

Transit lightcurve

3 out of the 4 regimes are trivial. Let’s cover the non-trivial one:

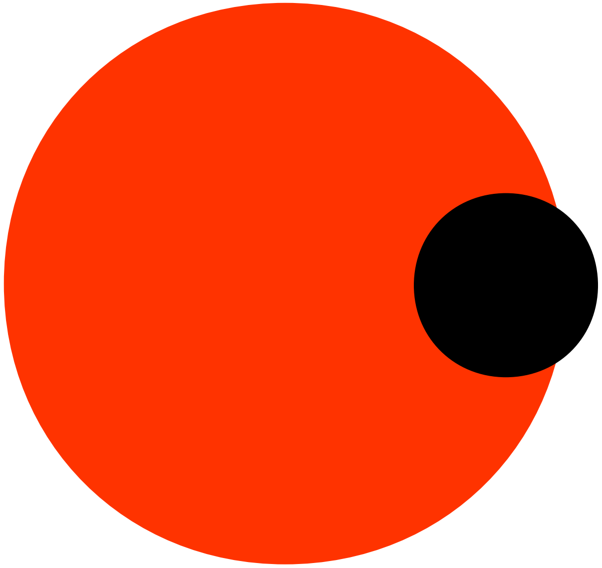

grazing transit

Transit lightcurve

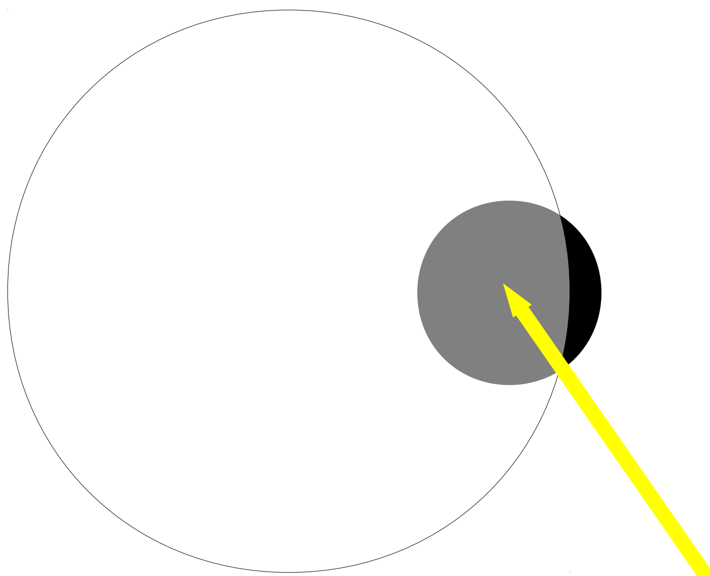

grazing transit

Flux determined by overlap region:
Intersection area of 2 circles

Transit lightcurve

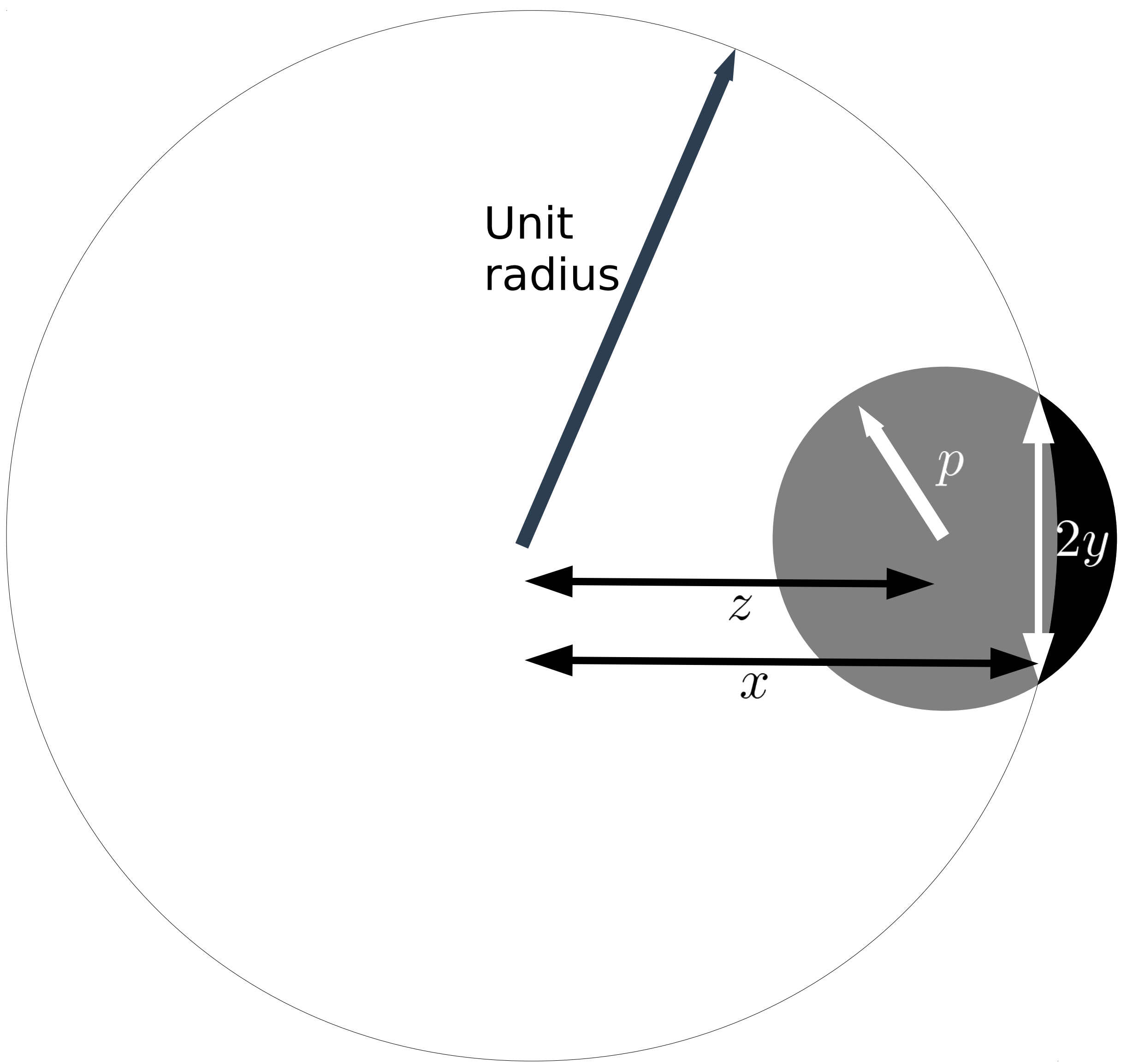

Let (x,y) origin be at centre of host. y points upwards.

All distances are in units of host radius (so host radius is unity)

Position of planet centre is (z,0)

Chord of intersection between host and planet has length 2y. Position of centre of chord is (x,0) and the top is (x,y).

Distance between chord and planet along x-axis is z-x (ie -ve when planet centre is to the left of chord, as in Figure)

Planet radius is p.

Transit lightcurve

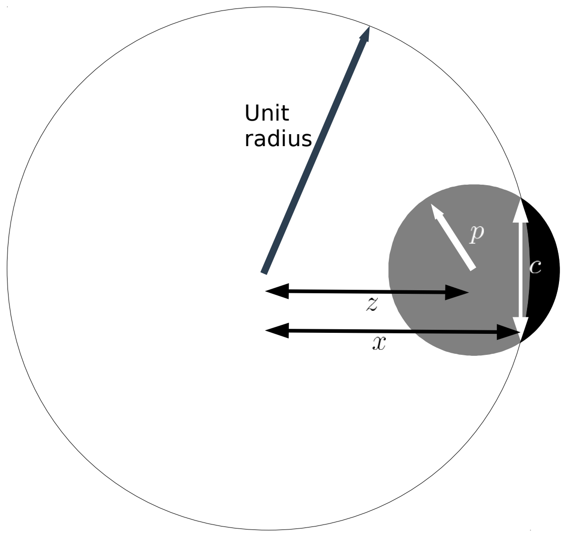

Equations of the host and planet circles, evaluated at the top of the chord, share common (*x*,*y*):

$$x^2 + y^2 = 1$$

$$(z - x)^2 + y^2 = p^2$$

$$\implies (z - x)^2 + (1 - x)^2 = p^2$$

Solve for x then use top equation to solve for y:

$$\implies x = \frac{1 - p^2 + z^2}{2z}; \quad y = \sqrt{\frac{4z^2 - (1 + z^2 - p^2)^2}{4z^2}}$$

Transit lightcurve

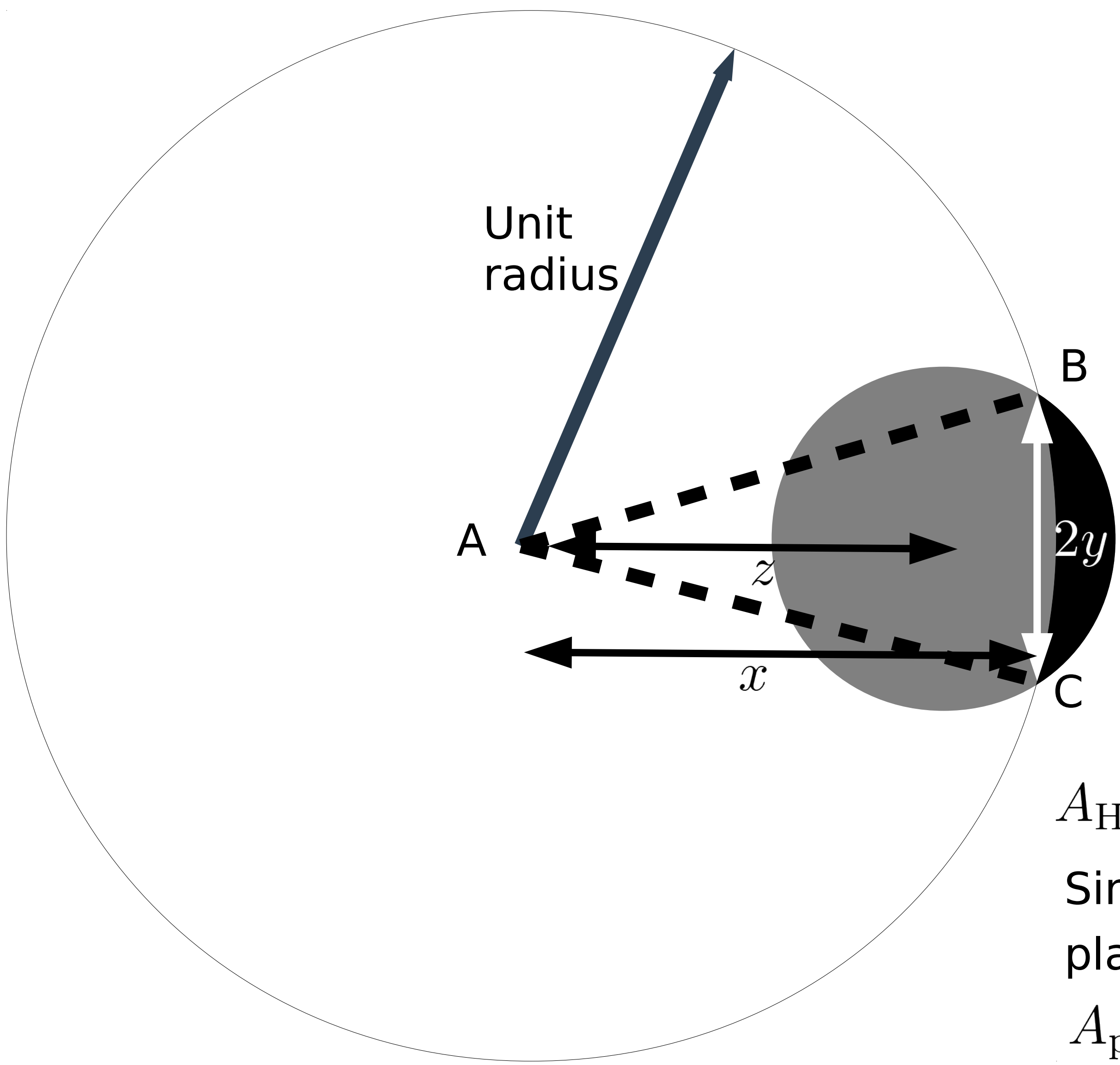

Overlap area is the sum of two lens-shaped areas:

- The (thin) area of the host lying to the right of the chord (A_H)
- The area of the planet lying to the left of the chord (A_p)

A_H is the difference in areas between the host area within circular wedge ABC and the triangle ABC

$$A_{\rm H} = \theta/2 - yx = \cos^{-1}(x) - yx$$

Similar exercise for A_p using *z-x* in place of *x:*

$$A_{\rm p} = p^2 \cos^{-1}[(z-x)/p] - y(z-x)$$

Transit lightcurve

Writing F_* as the host flux in units of its baseline (out-of-transit) flux, the transit flux can be written as

$$1 - F_* = \pi^{-1}(A_\mathrm{H} + A_\mathrm{p}) = \frac{1}{\pi}\{p^2 \cos^{-1}[(z-x)/p] + \cos^{-1}(x) - yz\}$$

Substituting in the formulae for *x* and *y* leads to the Mandel & Agol (2002) result:

$$1 - F_*(p, z) = \begin{cases} 0, & 1 + p < z, \\ \frac{1}{\pi}\left[p^2\kappa_0 + \kappa_1 - \sqrt{\frac{4z^2 - (1 + z^2 - p^2)^2}{4}}\right], & |1-p| < z \le 1 + p, \\ p^2, & z \le 1 - p, \\ 1, & z \le p - 1, \end{cases}$$

$$\kappa_0 = \cos^{-1}[(p^2 + z^2 - 1)/2pz], \quad \kappa_1 = \cos^{-1}[(1 - p^2 + z^2)/2z]$$

Transit lightcurve

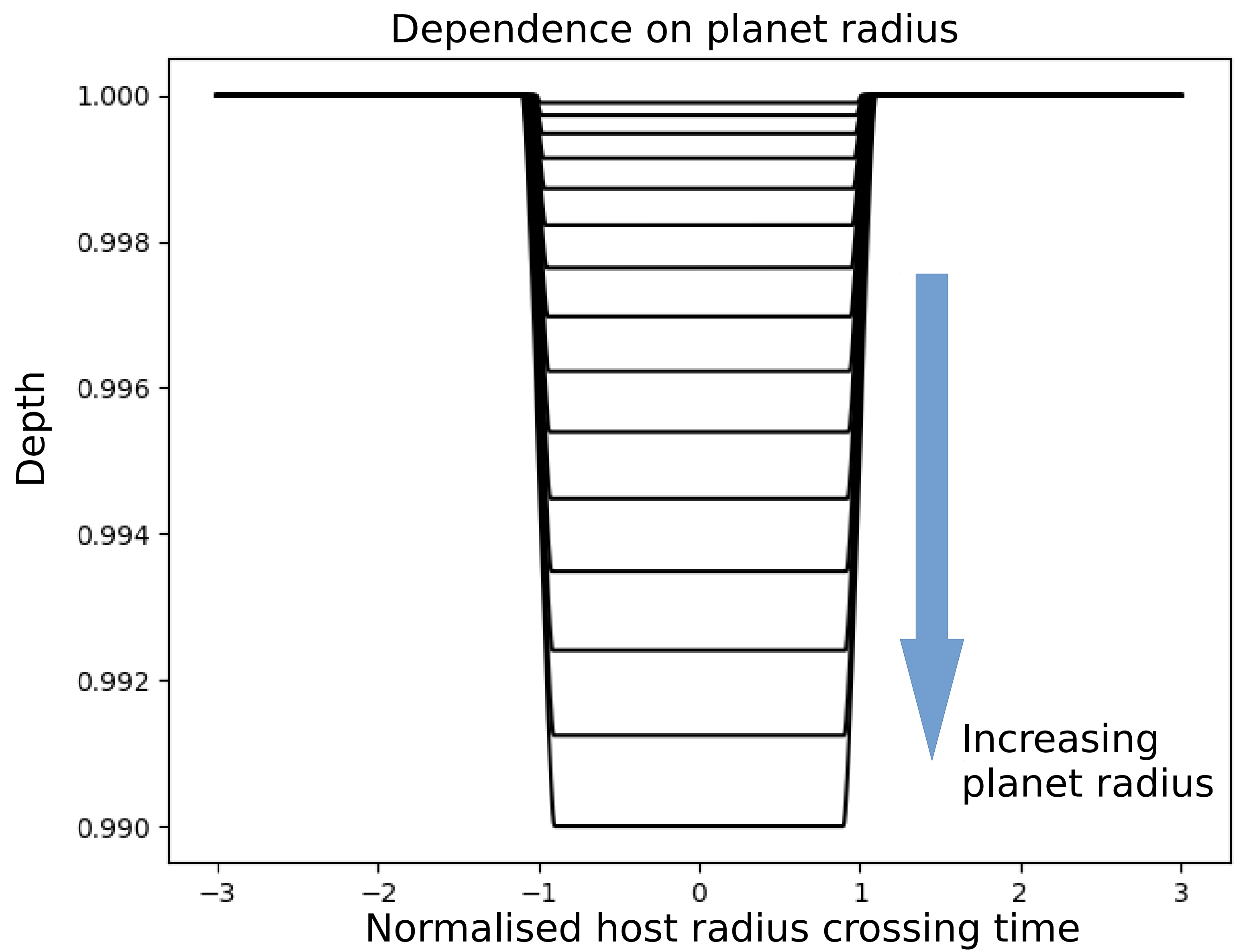

Transit lightcurve

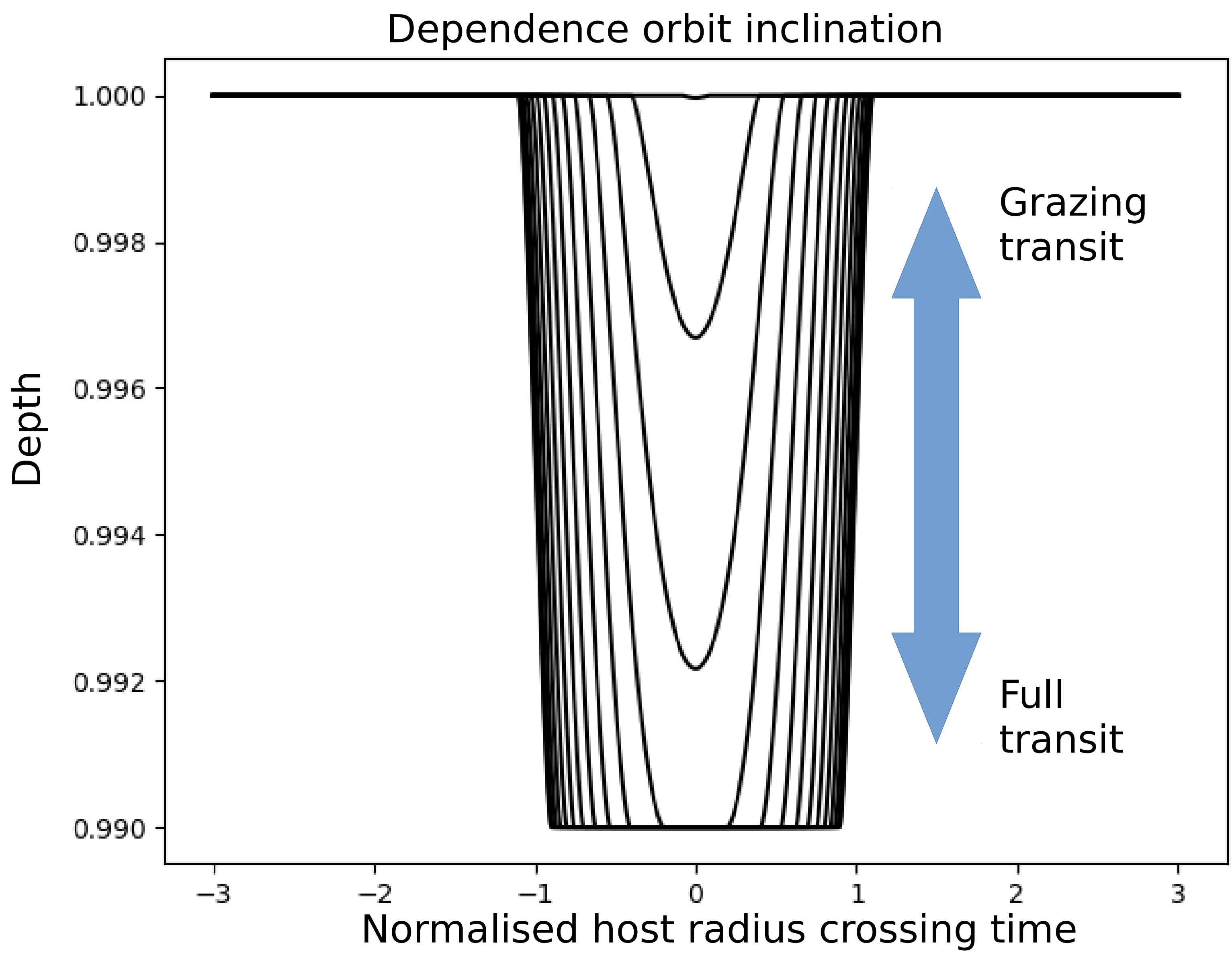

Transit lightcurve

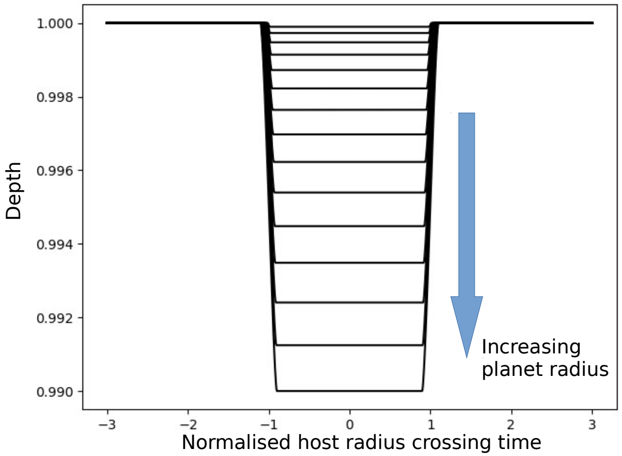

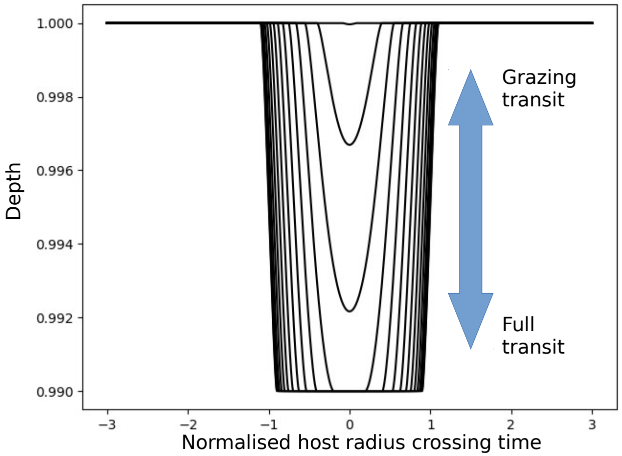

- For a uniform source transit inclination and depth are easy to decouple with reasonable data coverage.
- In optical bands hosts show limb-darkening: radially decreasing brightness
- Mandel & Agol (2002) also provide analytic formulae for common limb-darkening models:

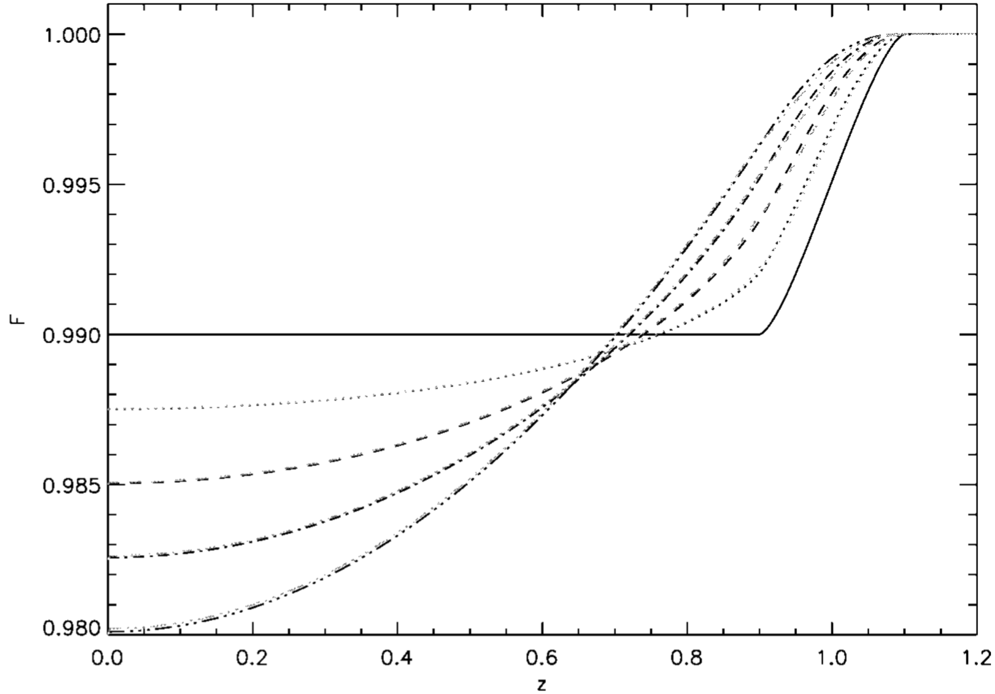

Transit parameters

- Basic transit photometry provides:
  - Radius of the planet in units of the host radius.
  - The orbital period P
  - The inclination angle i
  - The eccentricity e may sometimes be constrained
- But:
  - Basic transit photometry alone **cannot** determine the planet mass (only the size)!

Transit parameters

- Additional parameters (Seager & Mallen-Ornelas 2003) in the case of circular or **near-circular orbits**:

$$a/R_* = \frac{2P}{\pi} \frac{\Delta F_*^{1/4}}{(t_{14}^2 - t_{23}^2)^{1/2}}$$

(= inverse transit probability!)

$$\langle \rho_* \rangle = \frac{32}{G\pi} P \frac{\Delta F_*^{3/4}}{(t_{14}^2 - t_{23}^2)^{3/2}}$$

- application of a **host mass-radius** relationship can allow R_* to be estimated from $\langle \rho_* \rangle$, allowing R_p to be determined from the transit depth.
- Additional **data from RV** provides the planet mass M_p and therefore the planet average density $\langle \rho_p \rangle$
- **Limb darkening** coefficients provide additional stellar physics constraints

HD 209458b : first planet transit

Planet radius of 1.35 R_{Jup} and orbital period of 3.5 days.

A hot Jupiter orbiting a 1.1 $M_{\odot}$ star

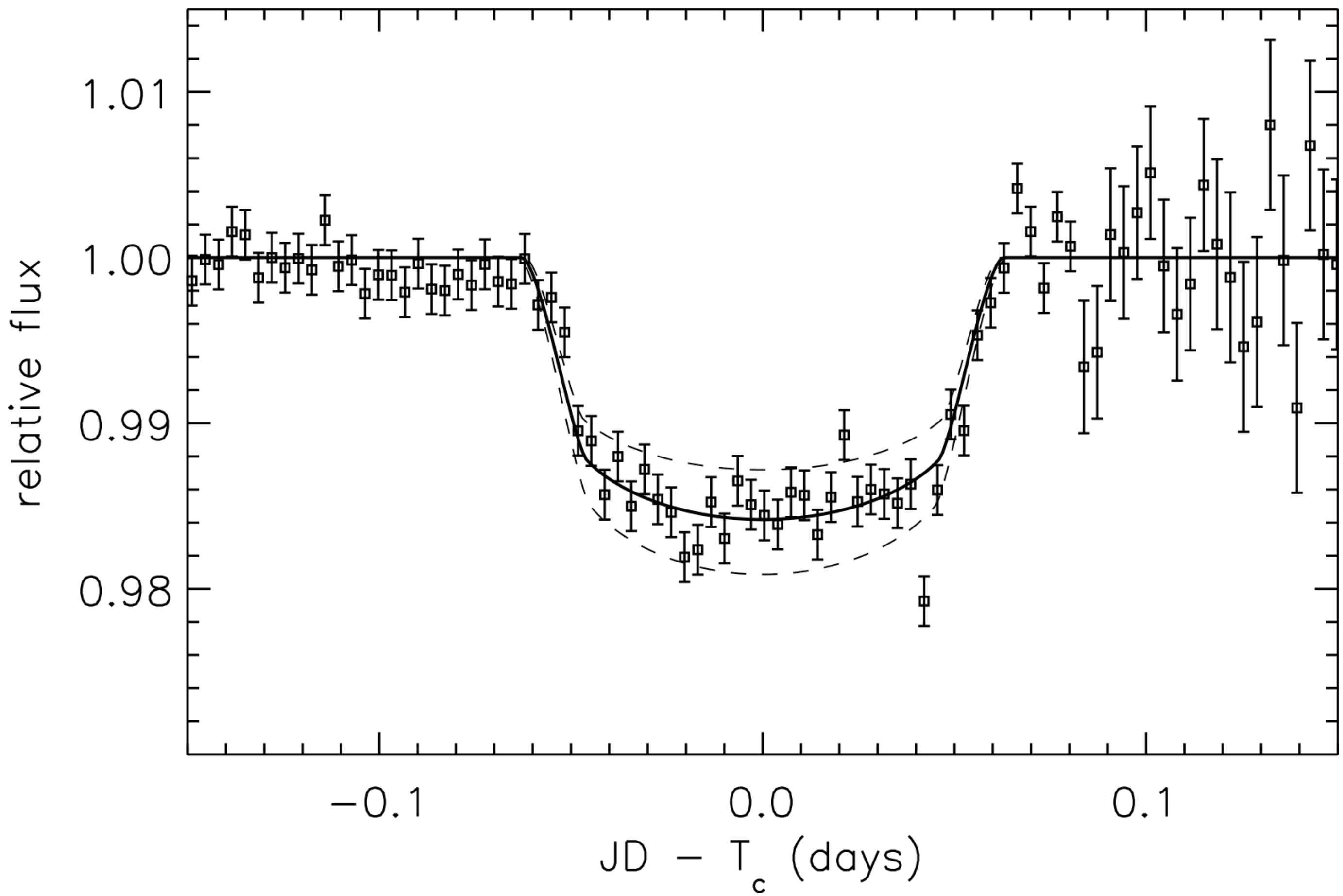

Original transit lightcurve from the discovery paper of Charbonneau et al (1999)

Transit duration

For a circular orbit in time Δt the planet sweeps an angle

$$\phi = 2\sin^{-1}(b/a) = \frac{2\pi\Delta t}{P} \qquad (12)$$

The path half-length across the host disk is [using Eq (1)]

$$b = \sqrt{R_*^2 - z^2} = \sqrt{R_*^2 - a^2\cos^2 i} \qquad (13)$$

which gives

$$\Delta t \simeq \frac{P}{\pi}\sin^{-1}\left[\frac{\sqrt{R_*^2 - a^2\cos^2 i}}{a}\right] \qquad (14)$$

as the **transit duration** for $R_p << R_*$ (ie ignoring ingress/egress times).

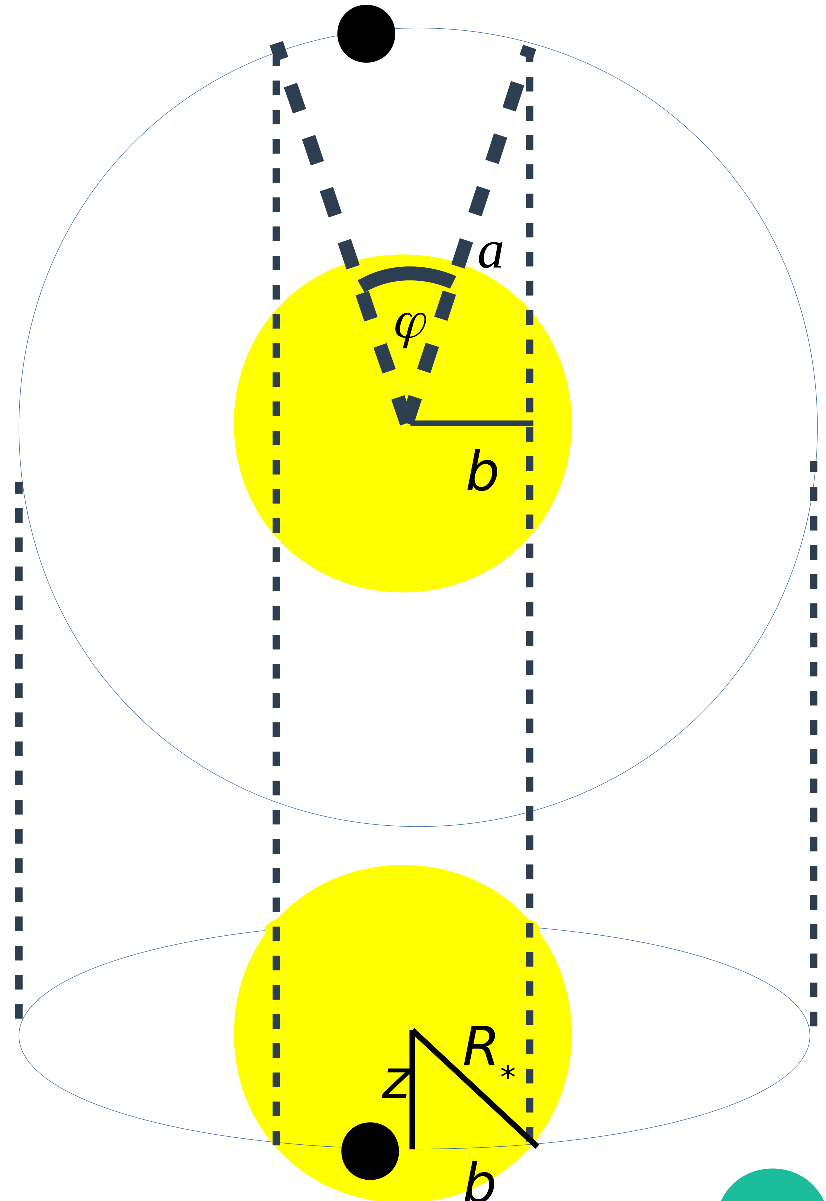

Dependence of transit signal on exoplanet parameters

- We have seen that the transit signal depends on the radius of the planet. The radius is correlated with mass M_p. For rocky (lower mass) planets we may expect a roughly characteristic planet density (for solar system rocky planets this is 4-5 g/cm^3), in which case $M_p \propto R_p^3$

- The precision of transit measurements, σ_T, for a single transit is governed by detecting a difference in the number of photons ΔN received during transit and out of transit. Since the photon error is governed by Poisson statistics we have

$$\sigma_T \propto (\Delta N)^{-1/2} \propto (F_* - F_{\min})^{-1/2} \propto R_p^{-1} \qquad (18)$$

Dependence of transit signal on exoplanet parameters

- The precision σ_T can be improved by observing multiple transits. For a fixed total observing time *T* and a planet with period *P* we can observe *n* = *T*/*P* transits. We can expect the precision to improve as

$$\sigma_T \propto n^{-1/2} \propto P^{1/2} \qquad (19)$$

- At some point σ_T will be reduced down to the level of systematic errors imposed by the telescope, atmosphere, host star stability or data reduction technique. At this point σ_T is fixed and so we can combine Eq (18) and (19) to see the trade off between exoplanet parameters

$$\sigma_\mathrm{T} \propto R_p^{-1} P^{1/2} \implies R_p \propto P^{1/2} \;\; (\text{at limiting } \sigma_T) \qquad (20)$$

Dependence of transit signal on exoplanet parameters

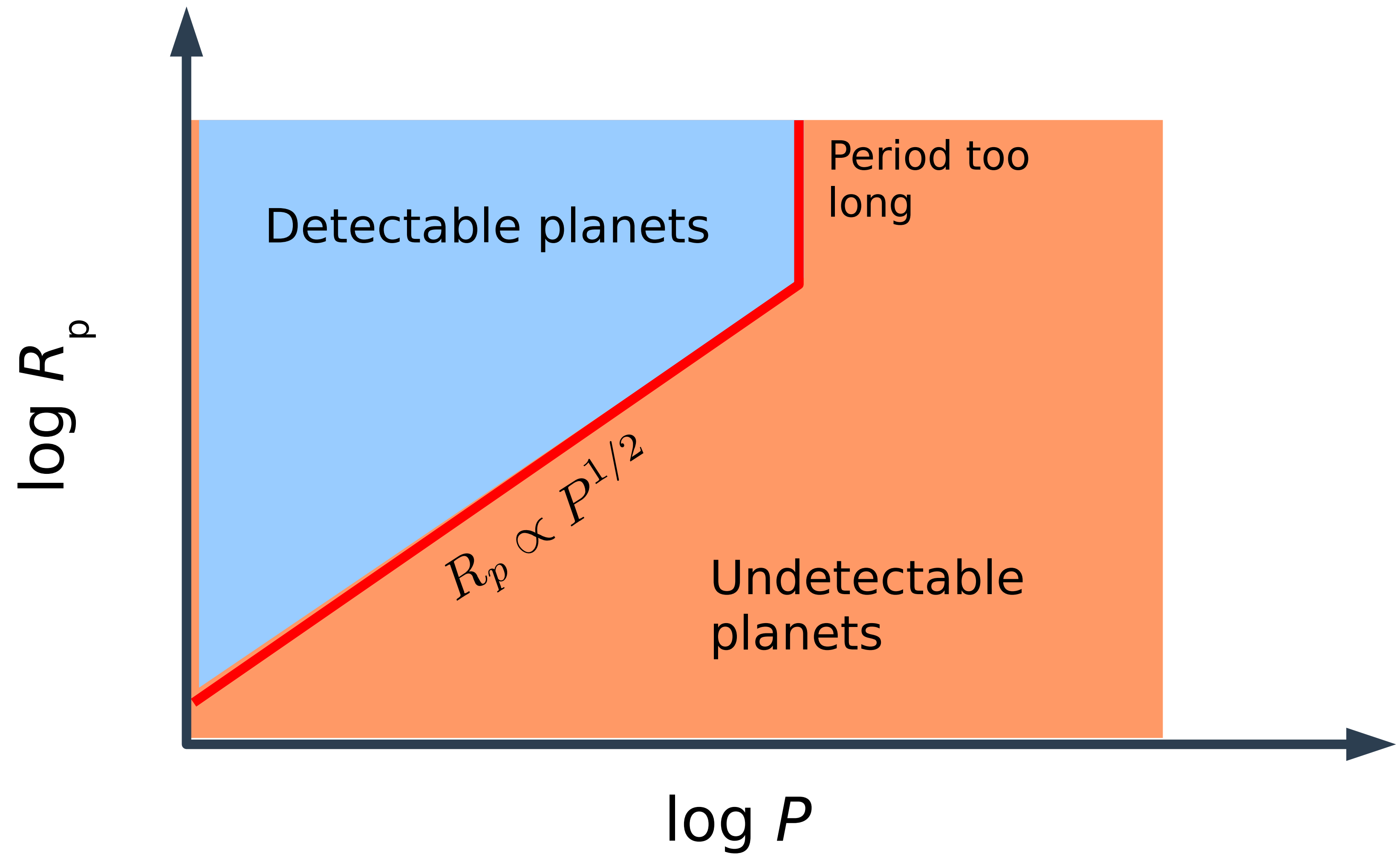

Dependence of transit signal on exoplanet parameters

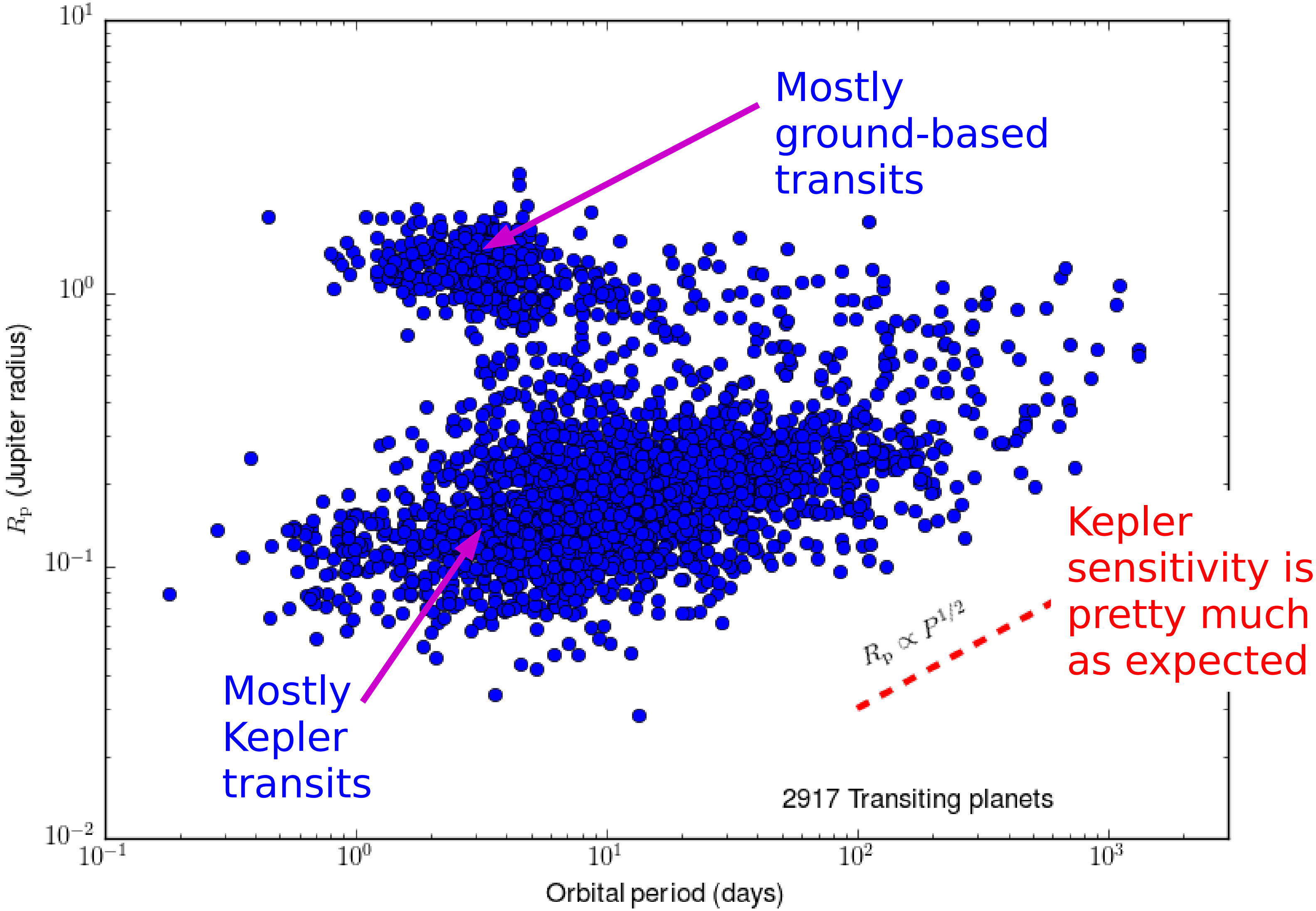

Kepler

MANCHESTER 1824
The University of Manchester

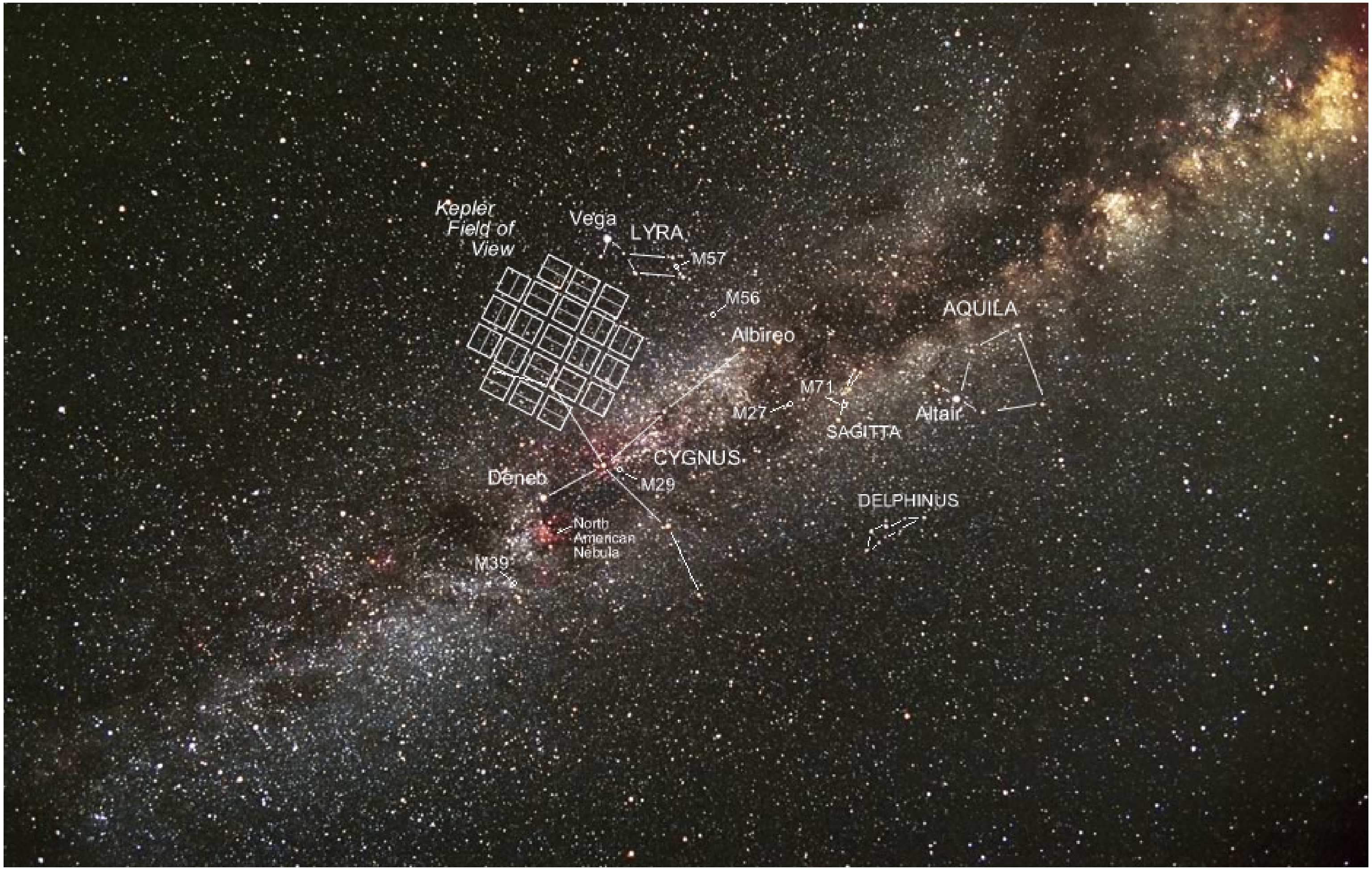

Source: kepler.nasa.gov

NASA space telescope which measured the brightness of 150,000 bright stars every 30 minutes. Sensitive to Earth-sized transits

Tres-2b as observed by Kepler

Kepler was capable of very precise photometry!

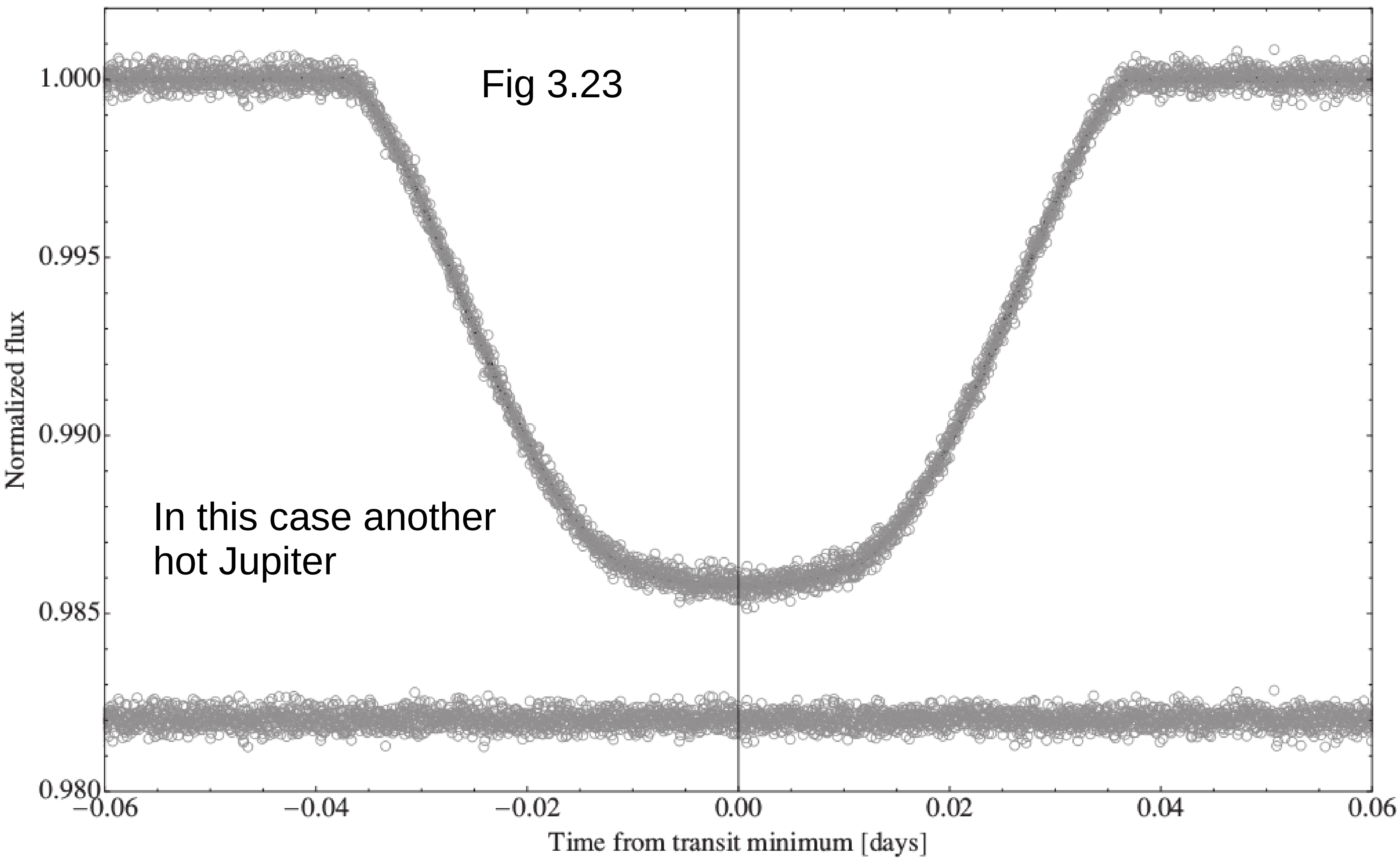

From Kipping & Bakos (2011)

Kepler

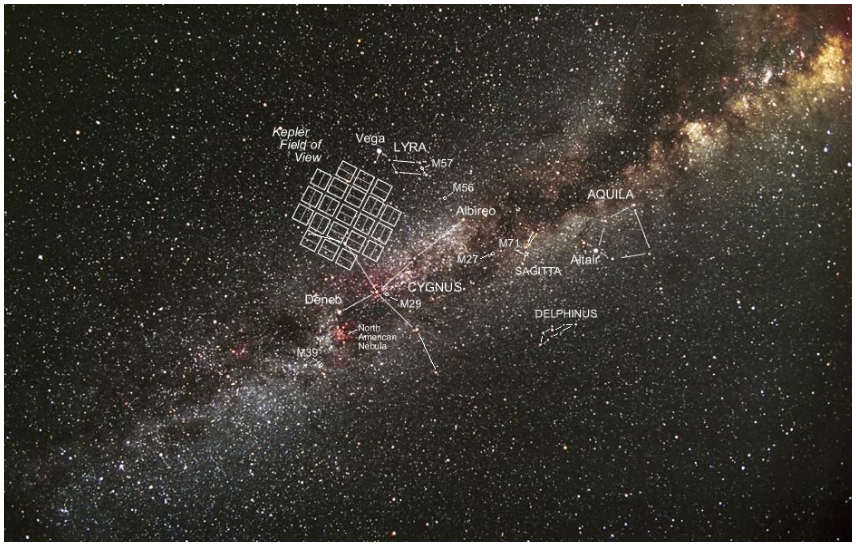

- Kepler has been a powerful observatory for exoplanet demography with sensitivity from sub-Earth sized planets upwards

- However, by focussing on a specific region, Kepler has to go deep to obtain large numbers of planets

- Many Kepler candidates are too faint to follow up from the ground, limiting the science potential of the Kepler dataset

- Ground-based surveys have tended to follow a wide and shallow strategy *eg SuperWASP) and this is now the stragety for current and future space-based missions too (TESS, PLATO)

TESS

Shallow, all-sky approach. Much more suitable for ground-based follow-up

Ground-based: NGTS

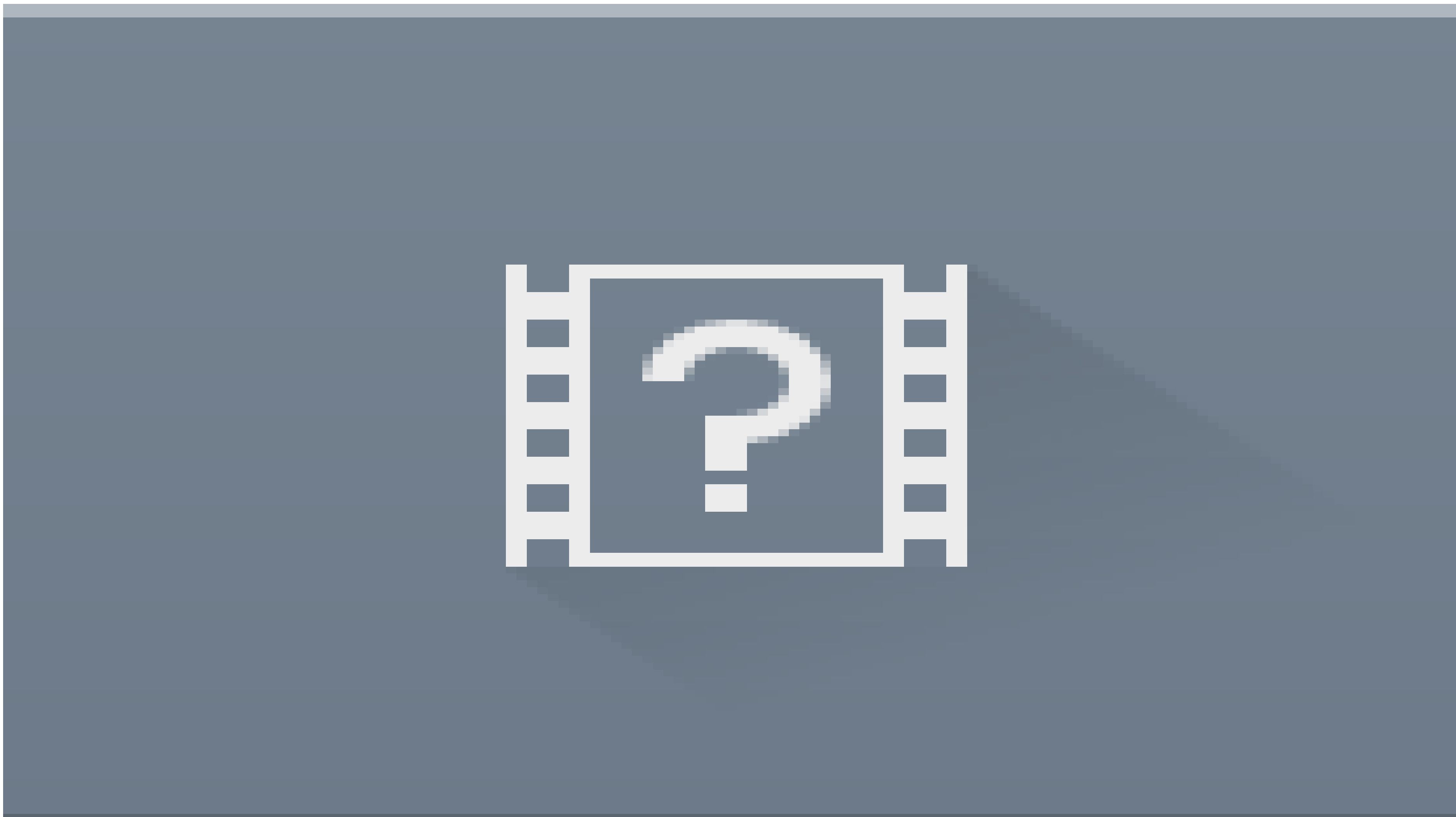

Complications

Seager & Mallen-Ornelas (2003)

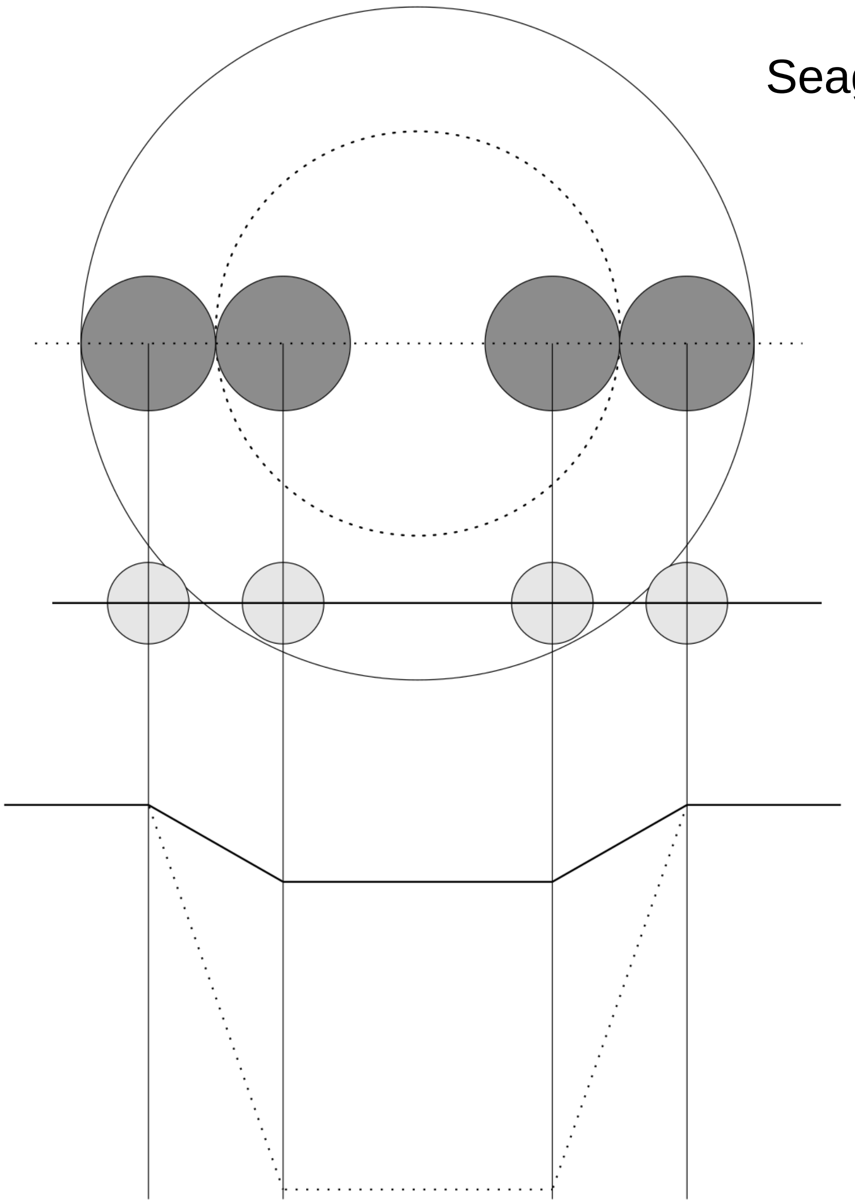

The presence of an unresolved background star can present a planet radius vs orbit inclination degeneracy

Complications

False positive signals can arise from unresolved distant eclipsing binary system contaminating the flux

Fig 3.28

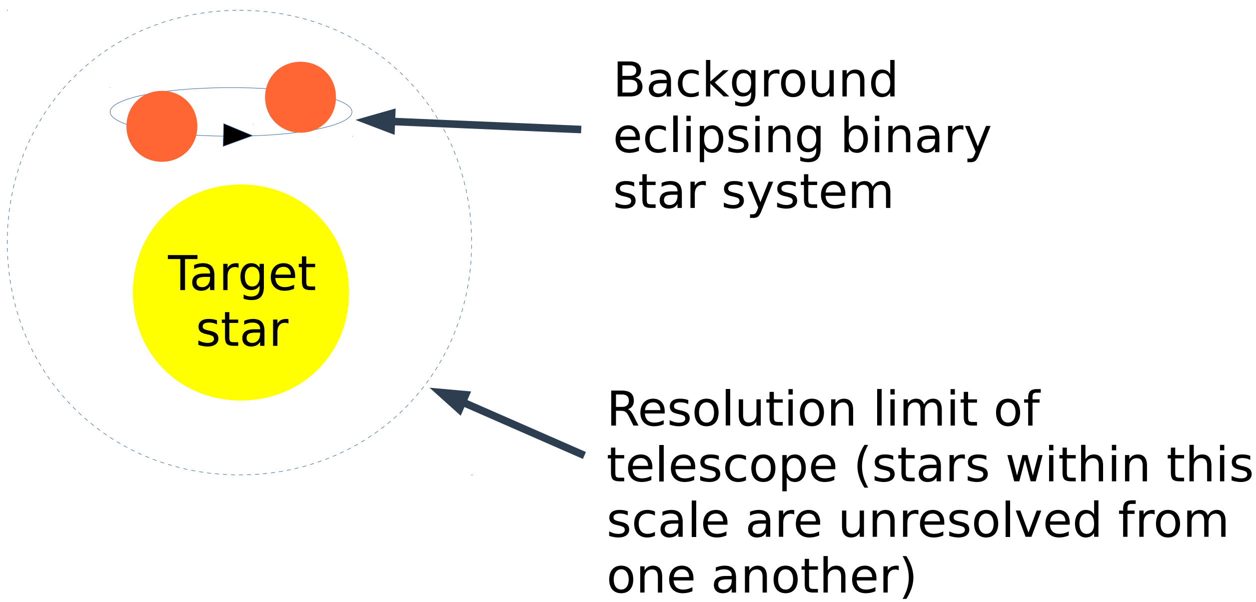

Complications

Intrinsic variability of the host star:

- long-term variability can be "de-trended" from the data by fitting for a general slope
- short-timescale periodic variability (e.g. star spots) can often be modelled as starspot periods are related to the stellar rotation rate
- short-term stochastic variability due to helioseismology sets a limit on the precision of transit detection. Surveys tend to pick "quieter" stellar types to minimize this

Trappist-1

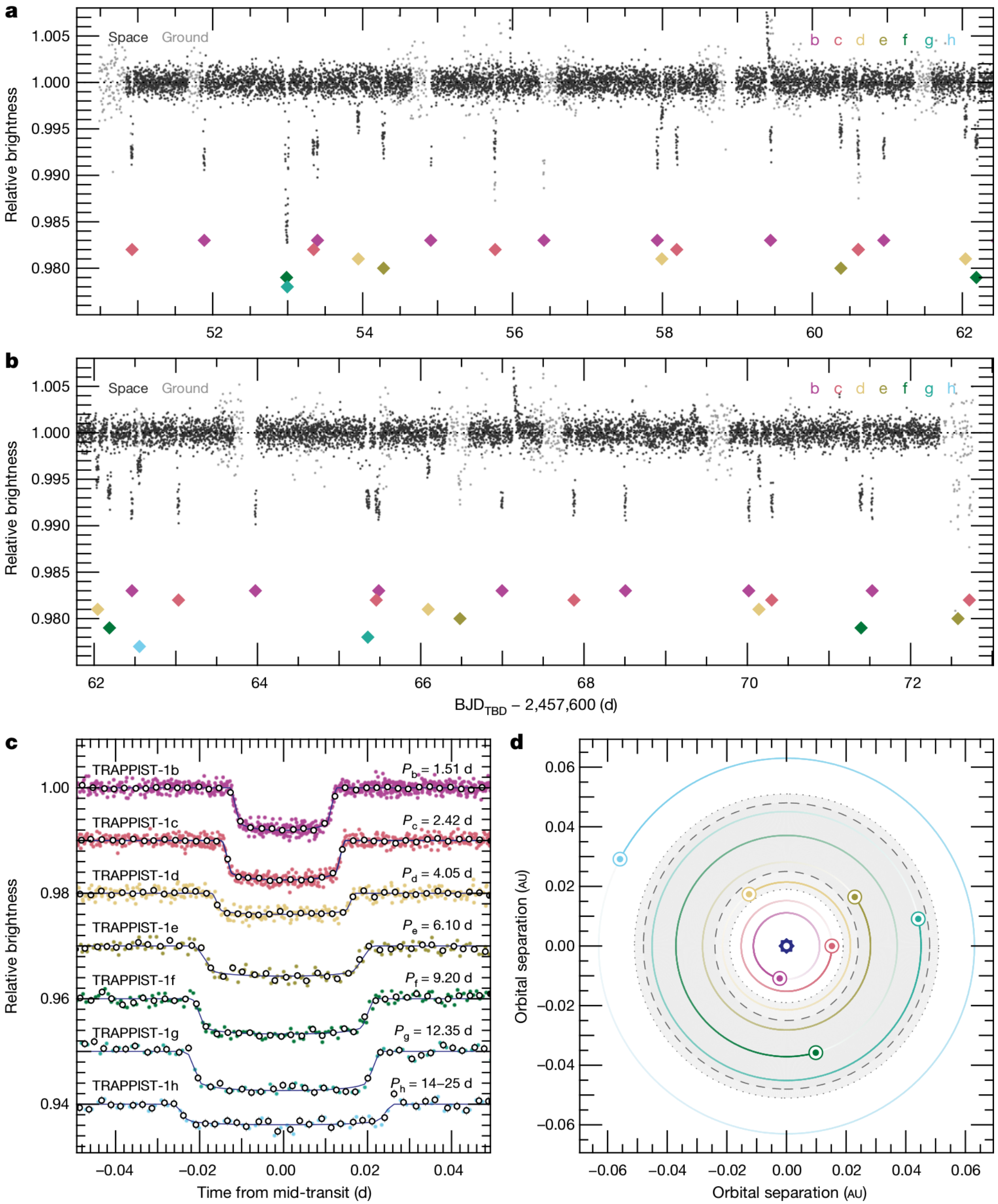

Gillon et al (2017)

A closely packed system of **seven** Earth-sized exoplanets orbiting low mass M dwarf star 12 pc away.

All may potentially be able to host liquid water

Trappist-1

Planets	b	c	d	e	f	g	h
Number of unique transits observed	37	29	9	7	4	5	1
Period, P (days)	$1.51087081 \pm 0.60 \times 10^{-6}$	$2.4218233 \pm 0.17 \times 10^{-5}$	$4.049610 \pm 0.63 \times 10^{-4}$	$6.099615 \pm 0.11 \times 10^{-4}$	$9.206690 \pm 0.15 \times 10^{-4}$	$12.35294 \pm 0.12 \times 10^{-3}$	20^{+15}_{-6}
Mid-transit time, $T_0 - 2{,}450{,}000$ (BJD_{TDB})	$7{,}322.51736 \pm 0.00010$	$7{,}282.80728 \pm 0.00019$	$7{,}670.14165 \pm 0.00035$	$7{,}660.37859 \pm 0.00038$	$7{,}671.39767 \pm 0.00023$	$7{,}665.34937 \pm 0.00021$	$7{,}662.55463 \pm 0.00056$
Transit depth, $(R_p/R_\star)^2$ (%)	0.7266 ± 0.0088	0.687 ± 0.010	0.367 ± 0.017	0.519 ± 0.026	0.673 ± 0.023	0.782 ± 0.027	0.352 ± 0.0326
Transit impact parameter, b ($R_\star$)	$0.126^{+0.092}_{-0.078}$	$0.161^{+0.076}_{-0.084}$	0.17 ± 0.11	$0.12^{+0.11}_{-0.09}$	0.382 ± 0.035	0.421 ± 0.031	$0.45^{+0.22}_{-0.29}$
Transit duration, W (min)	36.40 ± 0.17	42.37 ± 0.22	49.13 ± 0.65	57.21 ± 0.71	62.60 ± 0.60	68.40 ± 0.66	$76.7^{+2.7}_{-2.0}$
Inclination, i (°)	$89.65^{+0.22}_{-0.27}$	89.67 ± 0.17	89.75 ± 0.16	$89.86^{+0.10}_{-0.12}$	89.680 ± 0.034	89.710 ± 0.025	$89.80^{+0.10}_{-0.05}$
Eccentricity, e (2σ upper limit from TTVs)	<0.081	<0.083	<0.070	<0.085	<0.063	<0.061	-
Semi-major axis, a (10^{-3} AU)	11.11 ± 0.34	15.21 ± 0.47	$21.44^{+0.66}_{-0.63}$	$28.17^{+0.83}_{-0.87}$	37.1 ± 1.1	45.1 ± 1.4	63^{+27}_{-13}
Scale parameter, $a/R_\star$	$20.50^{+0.16}_{-0.31}$	$28.08^{+0.22}_{-0.42}$	$39.55^{+0.30}_{-0.59}$	$51.97^{+0.40}_{-0.77}$	$68.4^{+0.5}_{-1.0}$	$83.2^{+0.6}_{-1.2}$	117^{+50}_{-26}
Irradiation, S_p (S_{Earth})	4.25 ± 0.33	2.27 ± 0.18	1.143 ± 0.088	0.662 ± 0.051	0.382 ± 0.030	0.258 ± 0.020	$0.131^{+0.081}_{-0.067}$
Equilibrium temperature (K)‡	400.1 ± 7.7	341.9 ± 6.6	288.0 ± 5.6	251.3 ± 4.9	219.0 ± 4.2	198.6 ± 3.8	168^{+21}_{-28}
Radius, R_p (R_{Earth})	1.086 ± 0.035	1.056 ± 0.035	0.772 ± 0.030	0.918 ± 0.039	1.045 ± 0.038	1.127 ± 0.041	0.755 ± 0.034
Mass, M_p (M_{Earth}) (from TTVs)	0.85 ± 0.72	1.38 ± 0.61	0.41 ± 0.27	0.62 ± 0.58	0.68 ± 0.18	1.34 ± 0.88	-
Density, ρ_p (ρ_{Earth})	0.66 ± 0.56	1.17 ± 0.53	0.89 ± 0.60	0.80 ± 0.76	0.60 ± 0.17	0.94 ± 0.63	-

The table shows the values and 1σ errors for the parameters of TRAPPIST-1 and its seven planets, as deduced for most parameters from a global analysis of the Spitzer photometry, including *a priori* knowledge of the stellar properties. $M_\star$, $R_\star$, $\rho_\star$ and $L_\star$ are the stellar mass, radius, density and luminosity, respectively, given in units of the mass, radius, density or luminosity of the Sun ($M_\odot$, $R_\odot$, $\rho_\odot$, $L_\odot$). R_p, S_p, M_p and ρ_p are respectively the radius, irradiation, mass and density of the planet. BJD_{TBD}, barycentric Julian date in the barycentric dynamical time standard. Masses of the planets and upper limits on their eccentricities were deduced from the analysis of the TTVs (see text and Methods). We note that the planet TRAPPIST-1d does not correspond to the discarded 'TRAPPIST-1d' candidate presented in ref. 1 (see text).

†Informative prior probability distribution functions were assumed for these stellar parameters (see Methods).

‡Assuming a null Bond albedo.

Radii measured from transits, masses from TTV (see later in the course)

Gillon et al (2017)

Trappist-1

Mass and radius measurements means average internal density is known.

Consistent with Earth-like rocky planets

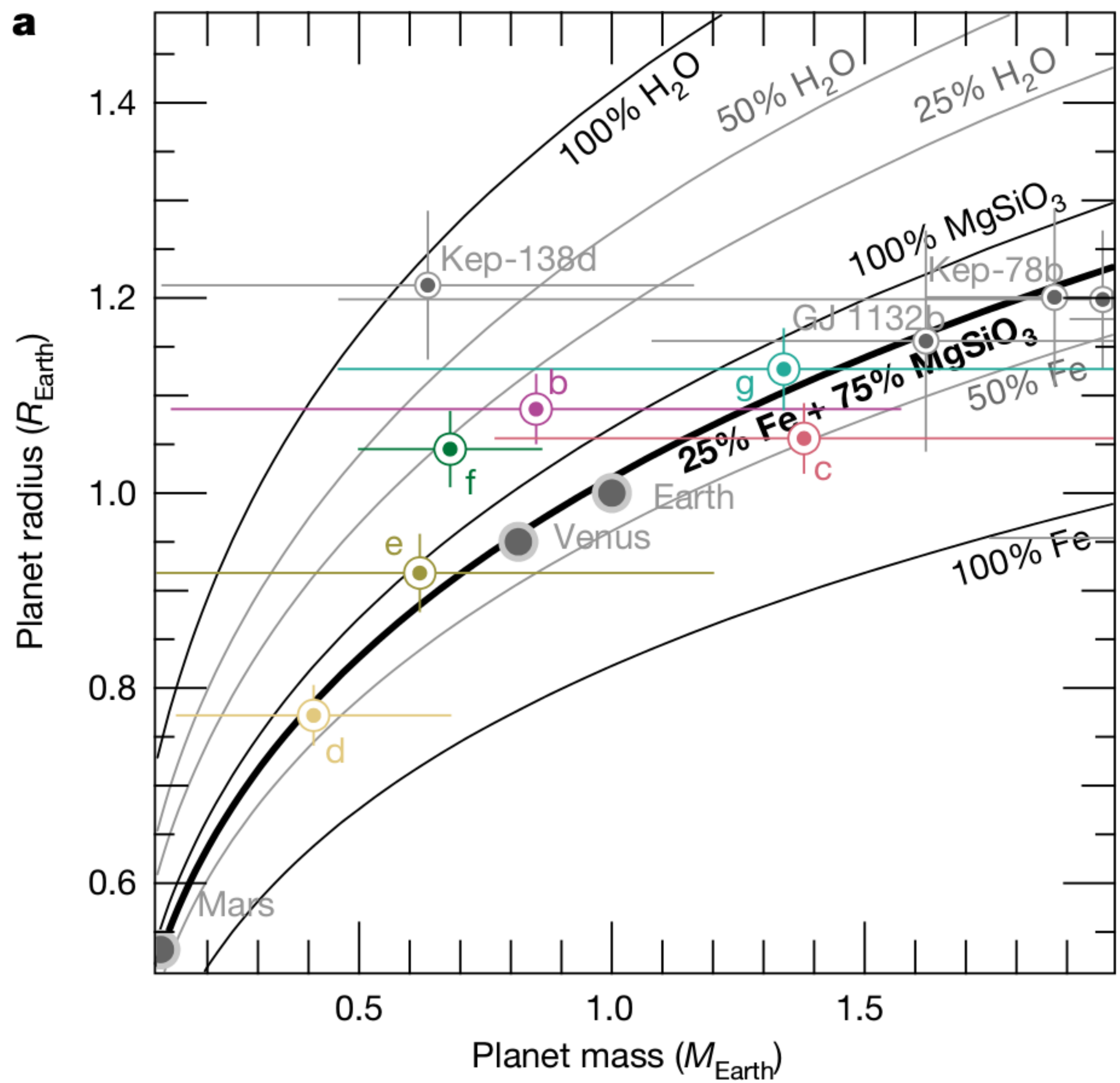

Gillon et al (2017)

Trappist-1

Host is much lower luminosity than the Sun but these planets are correspondingly closer in

Located at about the right region for liquid water to exist.

But we don't know whether it does on any of them.

Relatively nearby so amenable to atmospheric studies with HST/JWST/E-ELT in future...

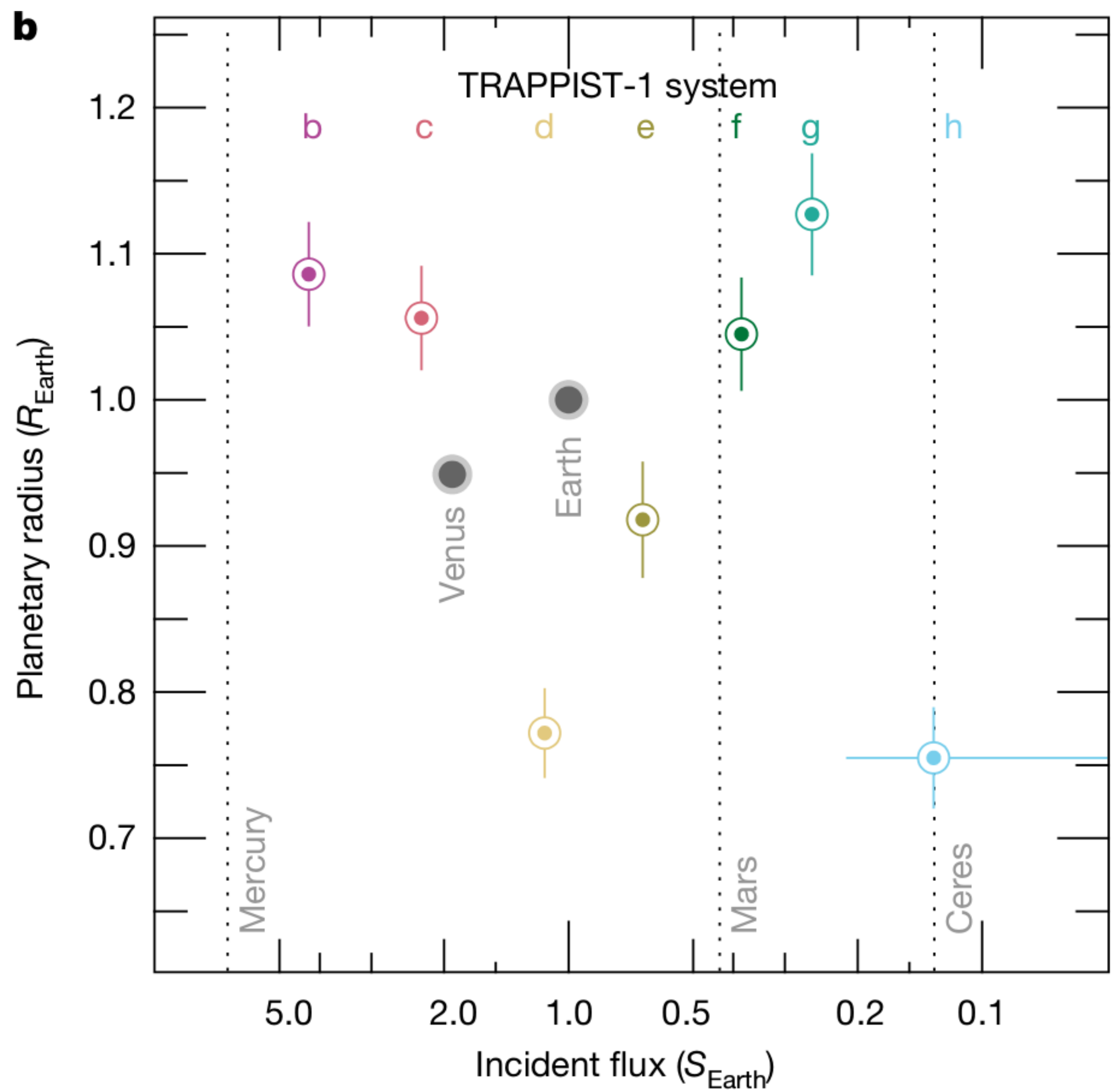

Gillon et al (2017)

Habitable zone planets

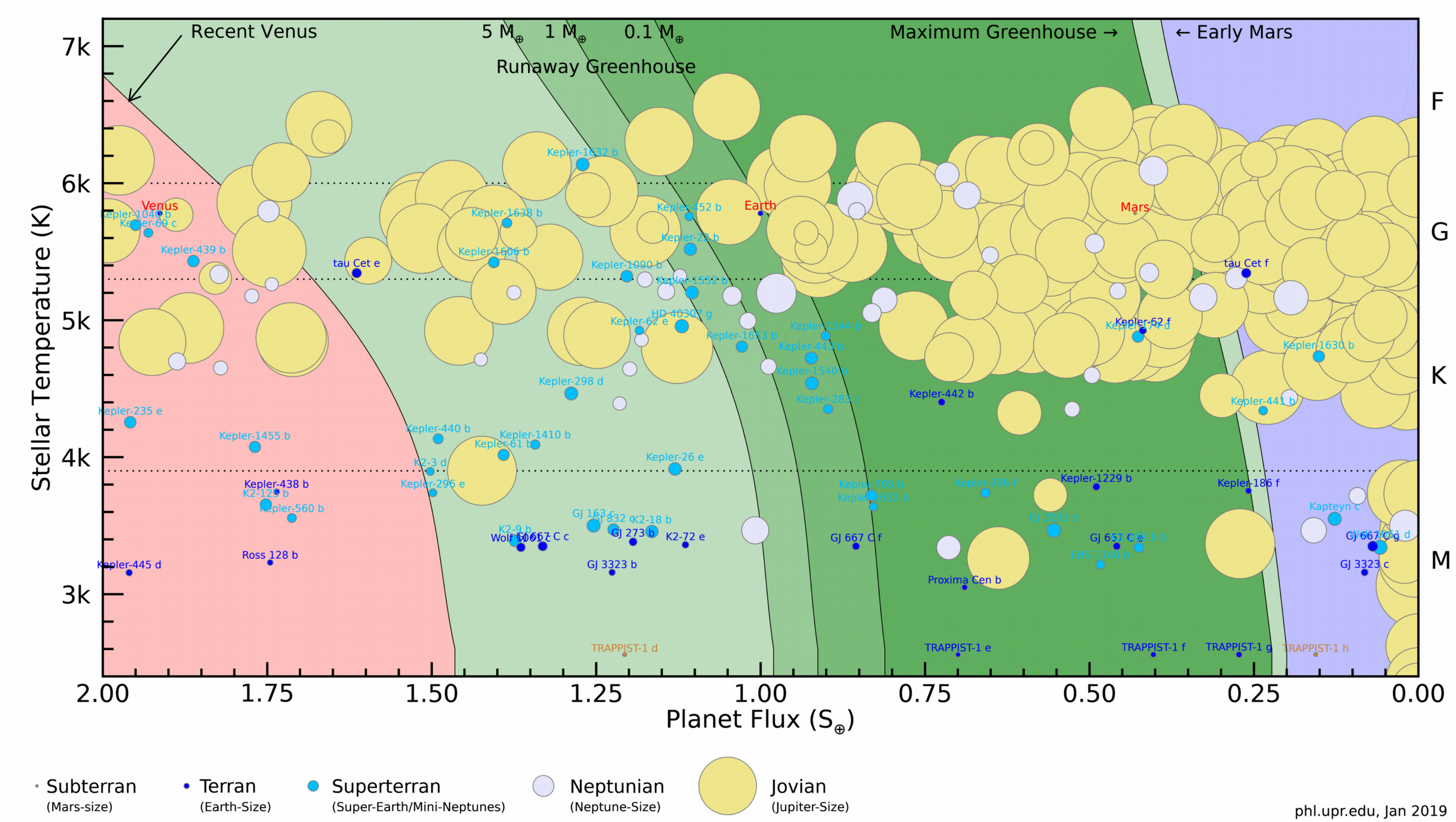

http://phl.upr.edu/

Circum-binary planets

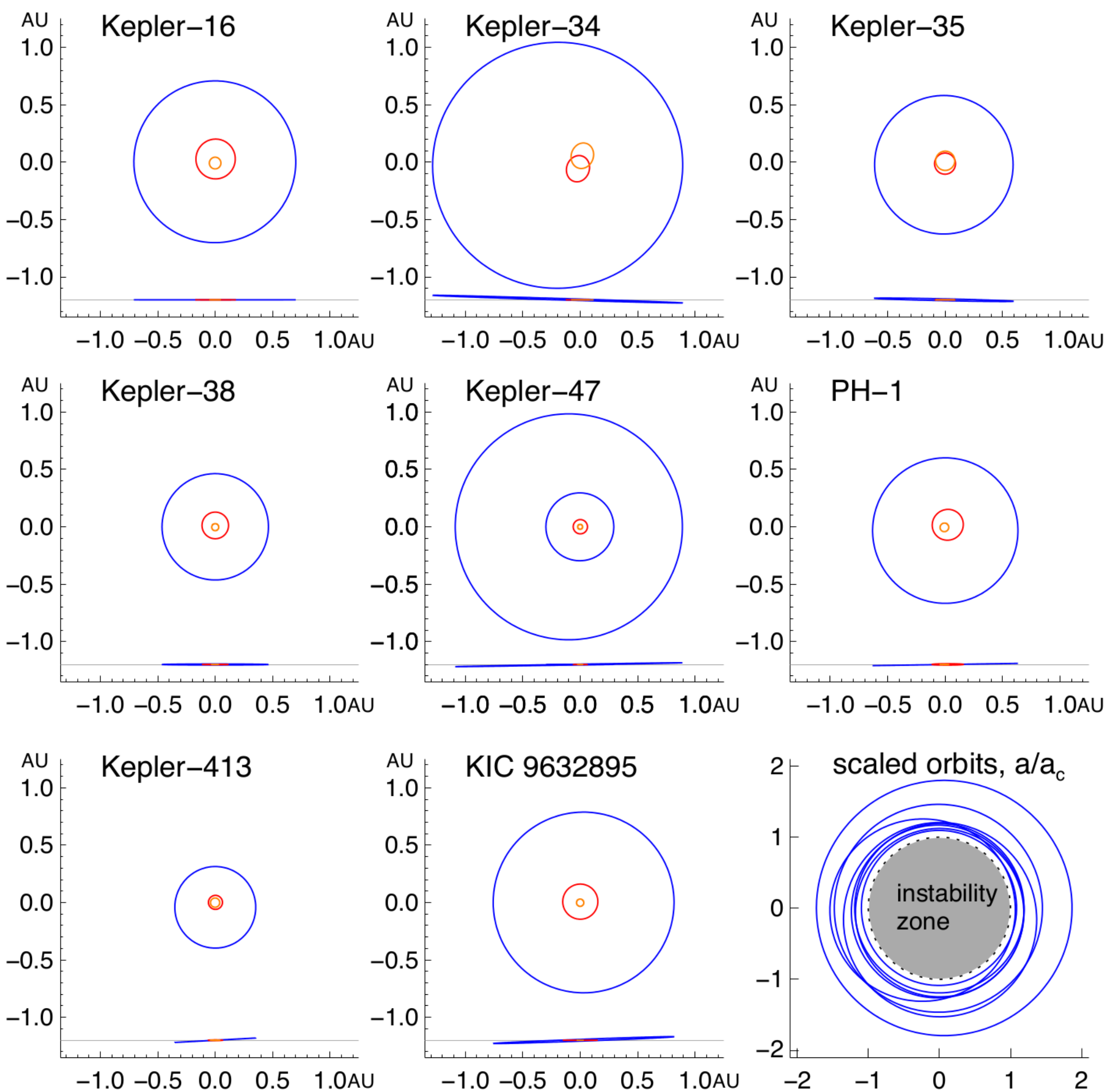

15 confirned stellar circumbinary planetary systems known to date.

Detected through transit, imaging and microlensing methods.

Shown are 8 candidates from Kepler:
orange circles = primary star orbit
red circles = secondary star orbit
blue circles = planet orbits
(Winn & Fabrycky 2015)

Transit planet demography

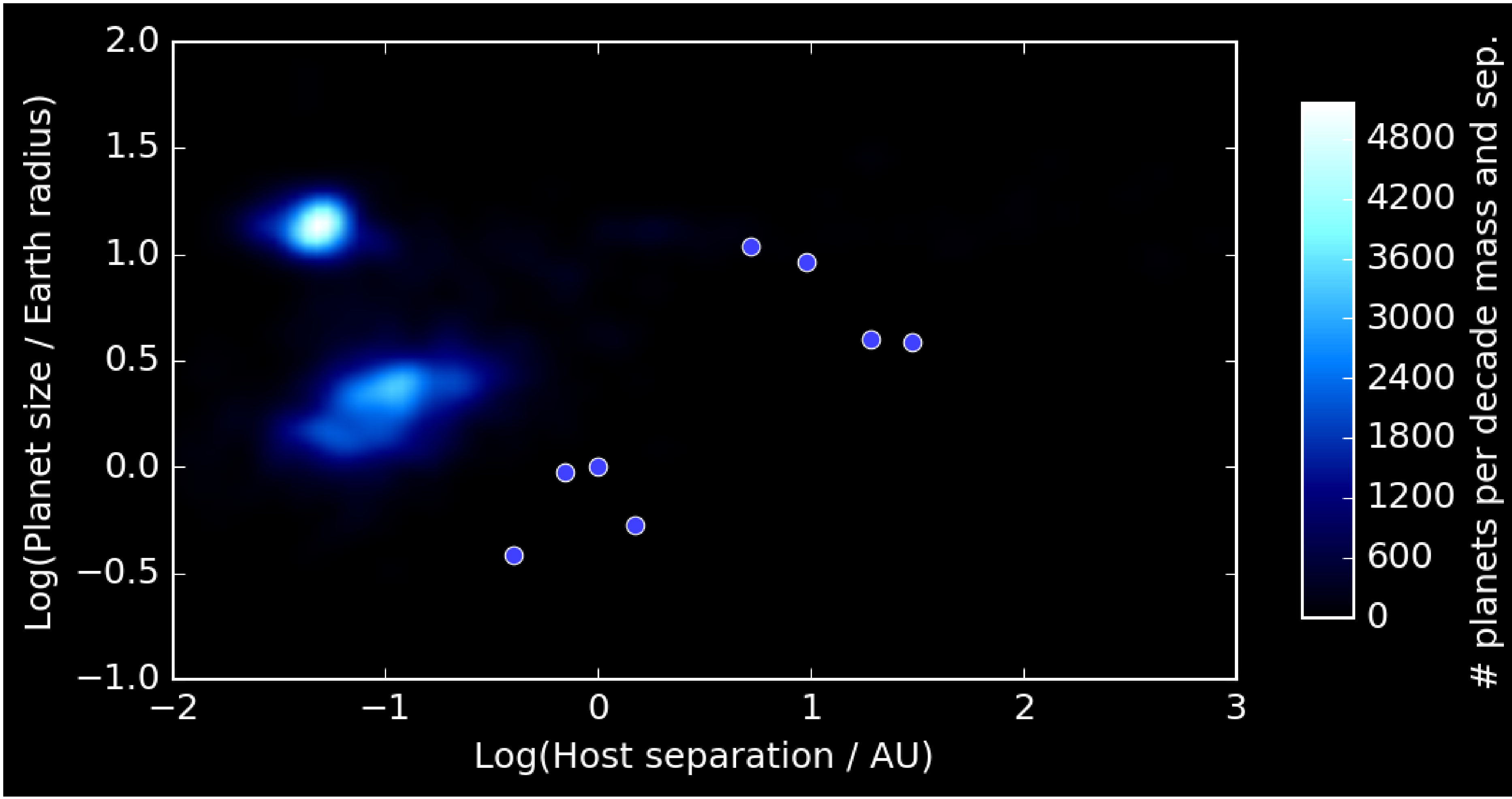

Demography landscape dominated by Kepler planets and hot Jupiters observed from the ground

Transit planet demography

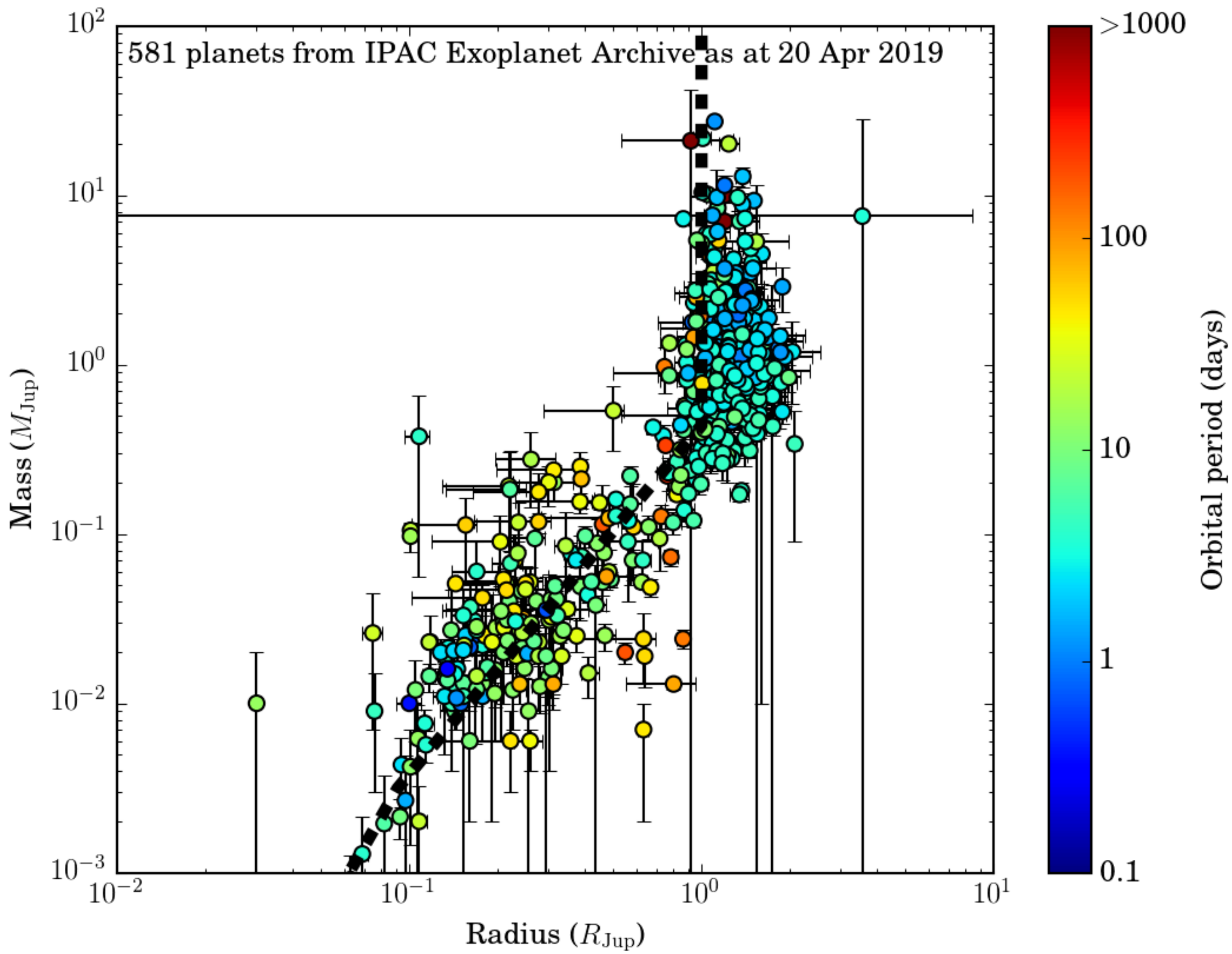

Transit planet demography

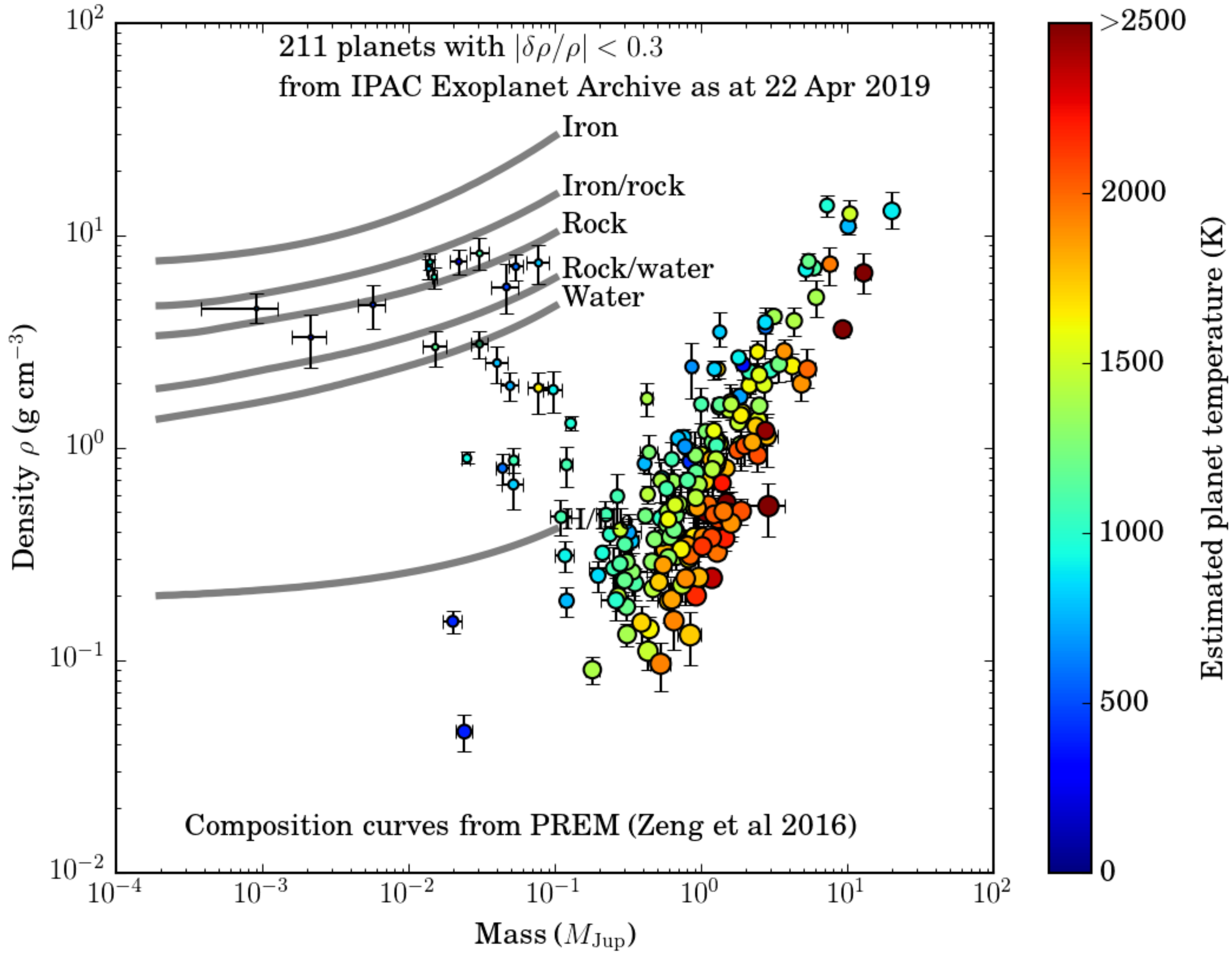

Transit planet demography

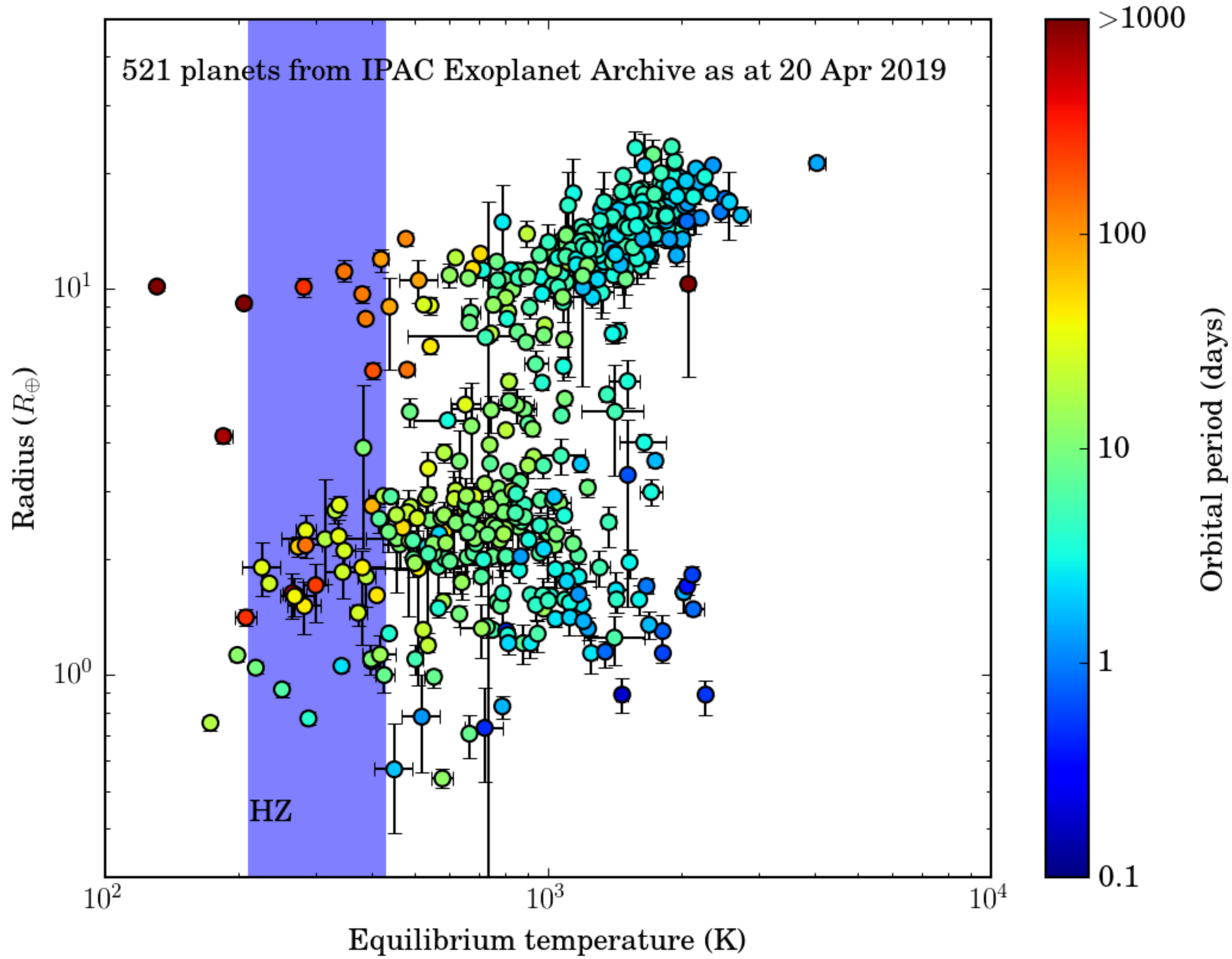

Assumes HZ temperature range equating to 0.75-1.7 AU for the Solar system

Transit timing variation (TTV)

The periodicity of a transit can be affected by several factors, including:

- The gravitational influence of another planet, especially in the case of **mean motion orbital resonance**
- Planet or host star tidal effects
- Transit around a binary star system (circum-binary exoplanet)
- Precession of periapsis due to General Relativistic effects
- **The presence of moons around the planet**

Orbital resonance effects

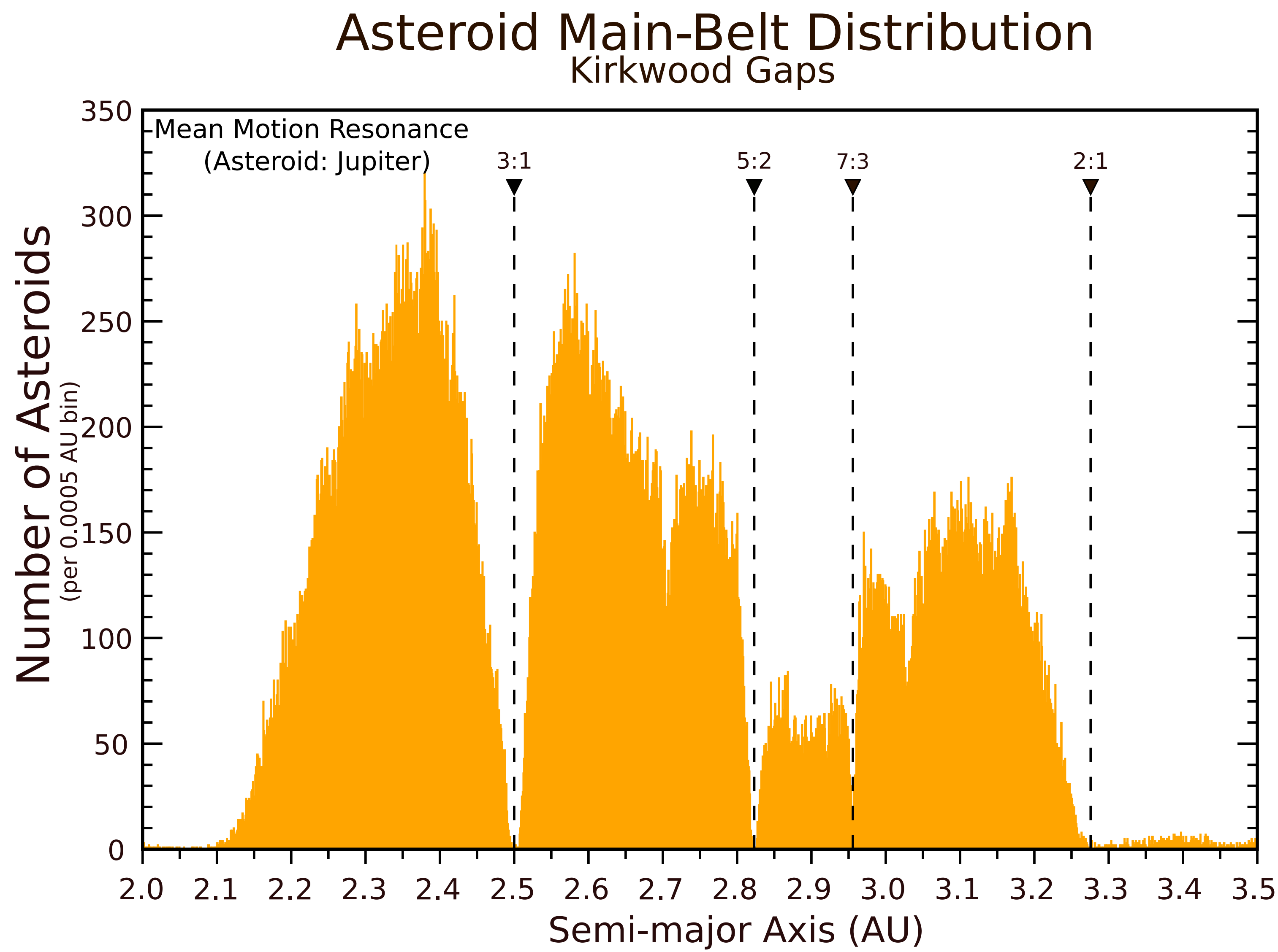

Fig 3.30

Alan Chamberlain, JPL/Caltech

Mean motion orbital resonance

Orbital resonance refers to where the orbital periods P_1 and P_2 of two bodies obey a simple small-integer relation

$$\frac{m}{P_1} - \frac{n}{P_2} = 0 \quad \text{(for small integers } m, n) \qquad (21)$$

Solar system examples:

- 3:2 orbital resonance between Neptune and Pluto
- Large orbital gaps in the main asteroid belt are associated with orbital resonances with Jupiter.
- Gaps in the Saturnian ring system are linked with orbital resonances with some of its moons

TTV signal from orbital resonance

A periodic variation in the transit ephemeris is predicted when a pair of planets have periods P_1 and P_2 which are close to (but not exactly) in a mean motion orbital resonance. Specifically, the TTV period is given by [c.f. Eq (21)]

$$\frac{1}{P_{\rm TTV}} = \left| \frac{m}{P_1} - \frac{n}{P_2} \right| \qquad \text{(for integers } m, n\text{)} \qquad (22)$$

Where $|m\text{-}n| = N$ we say that the resonance is an Nth-order resonance.

TTV due to orbital resonance

For transiting exoplanets, orbital resonances induce a periodic change in orbital speed which manifests as a modulation in the timing (ephemeris) of their transits.

Fig 3.31

NASA Kepler team movie illustrating TTV from a two-planet system exhibiting a 2:1 mean motion orbital resonance. Transit timing of the inner planet can be used to infer or confirm the presence of the outer planet, even if no transit is observed from it.

Kepler-19c: TTV discovery

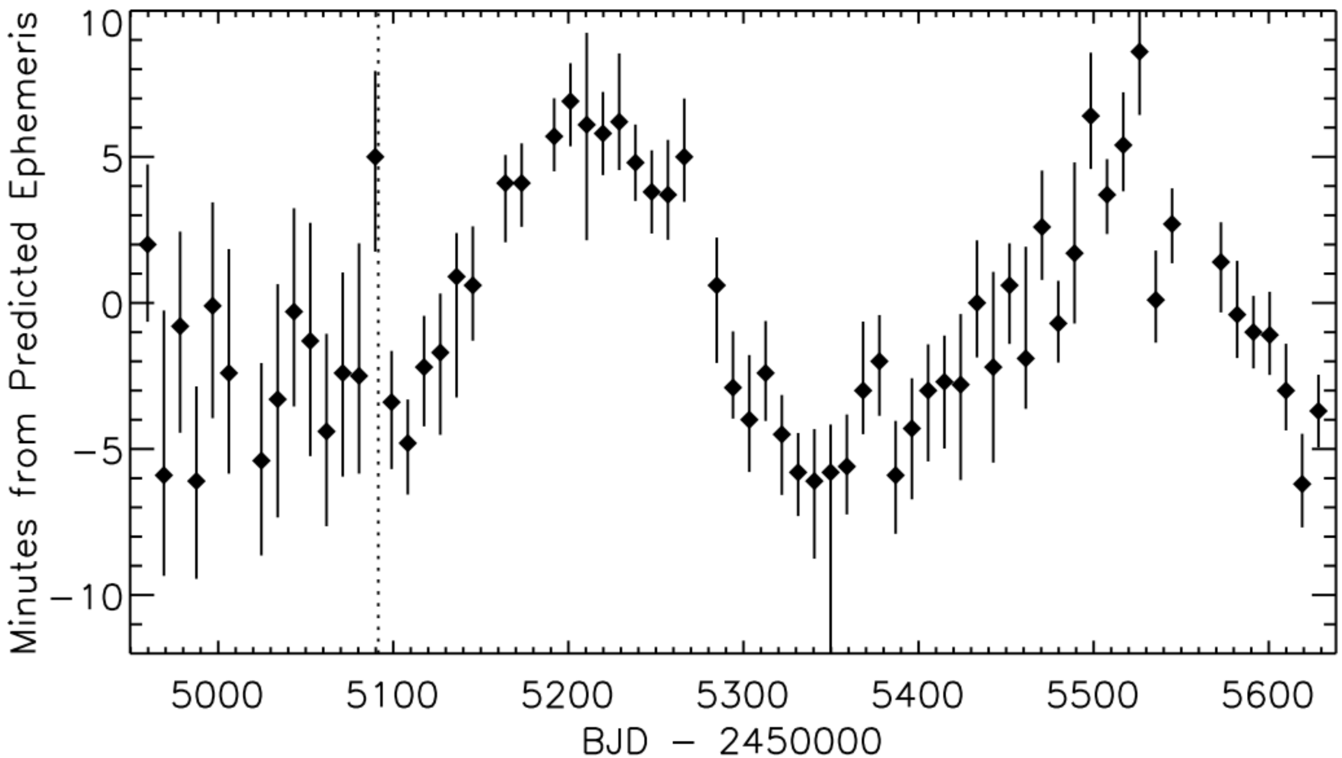

Fig 3.32

Ballard et al (2011)

Kepler timing of transiting exoplanet Kepler-19b reveals periodic variation due to a planet (Kepler-19c) with an orbit P < 160 days and mass $M_p < 6\ M_{Jup}$. No evidence of a transit by Kepler-19c was identified. The resonance between Kepler-19b and 19c is higher than first order.

Exomoons

- Just as planets in our Solar System possess moons we shoud expect exoplanets to host exomoons
- Timing variations of planet transits offer one of the best ways to discover an exomoon.
- Two types of timing signal:
  - transit timing variation (TTV)
  - transit duration variation (TDV)
- Detection of both TTV and TDV signal can confirm the presence of an exomoon (Kipping 2009)

TTV due to an exomoon

TTV signal can arise from the presence of an exomoon

Fig 3.33

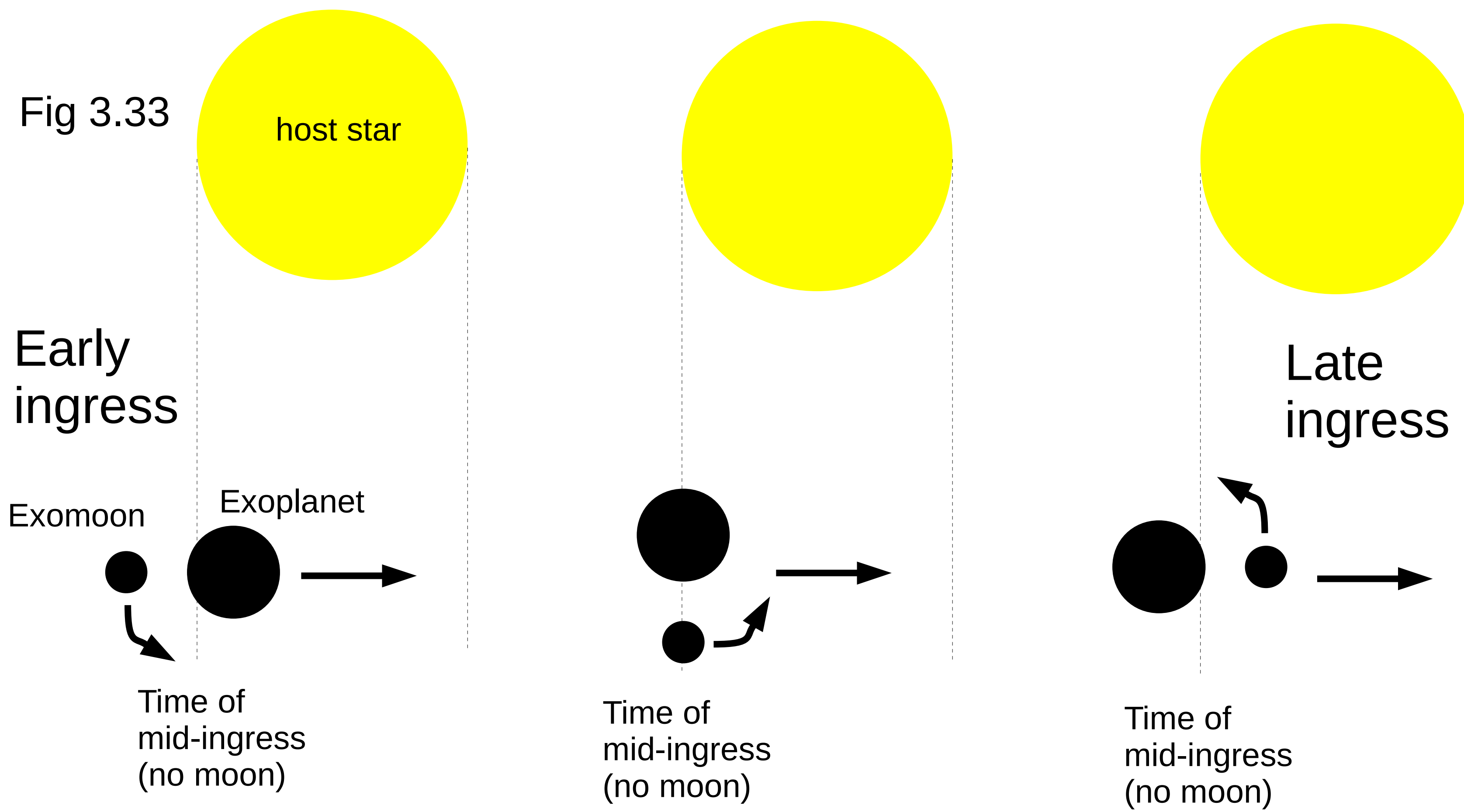

The time of ingress is determined by the position of the exoplanet relative to the exoplanet-exomoon barycentre

TDV due to an exomoon

Fig 3.34

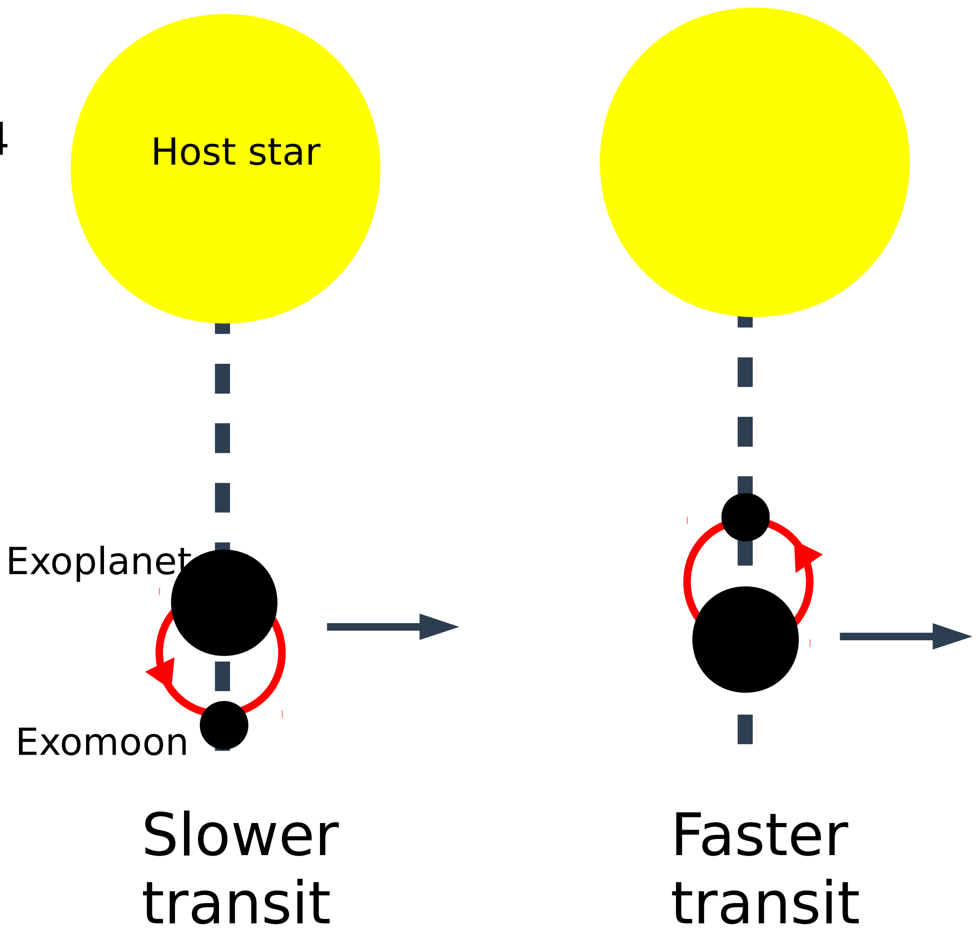

The duration of transit is modified by the orbit effect of the exomoon around the planet host

Exomoons with TTV/TDV

TTV and TDV signals should be out of phase by π/2 if the exomoon and exoplanet orbits are coplanar. The combination of TTV and TDV signals exhibiting such a phase difference is basically the key signature needed to confirm an exomoon.

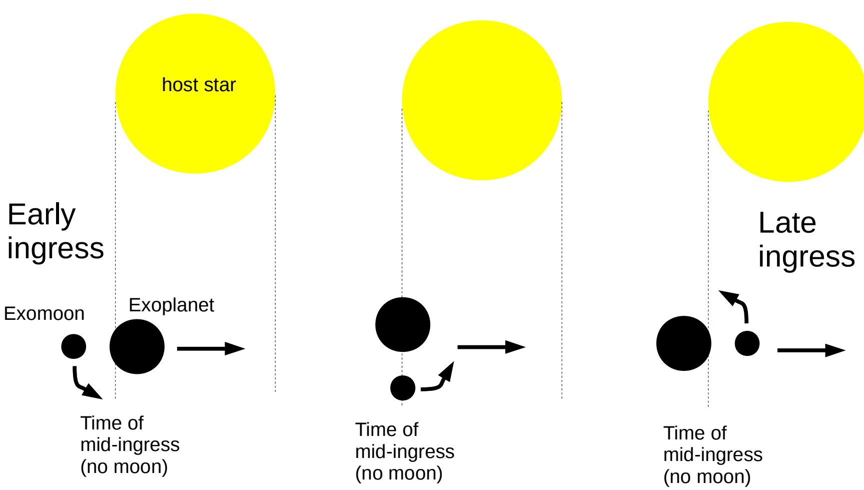

TTV

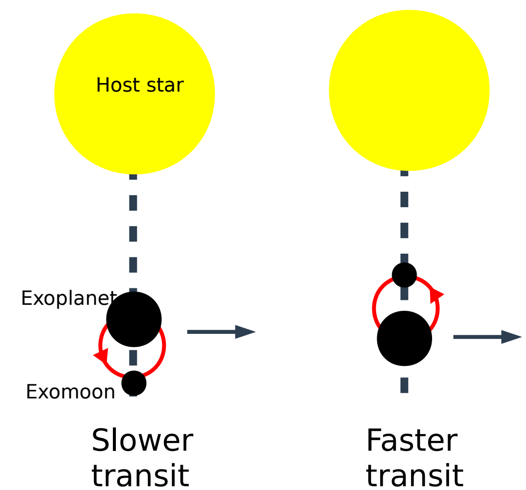

TDV

TTV + TDV exomoon signals

Fig 3.35

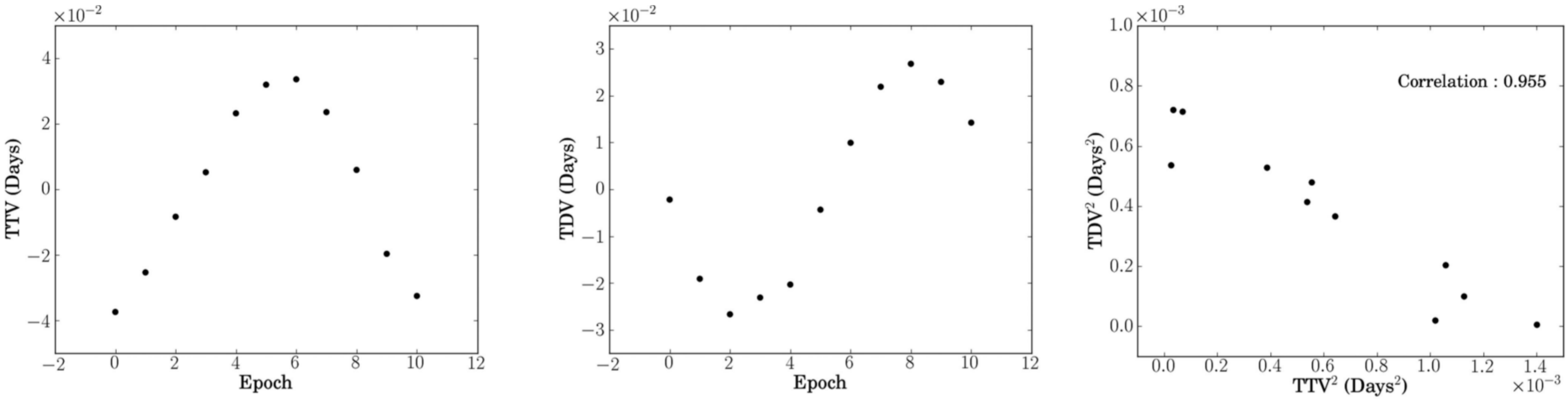

Simulated TTV and TDV signals of an Earth-mass exomoon and Jupiter host planet orbiting in the habitable zone of an M-dwarf host star (Awiphan & Kerins 2013)

TTV and TDV signals should exhibit a strong correlation for a genuine exomoon signal

Planet atmospheres

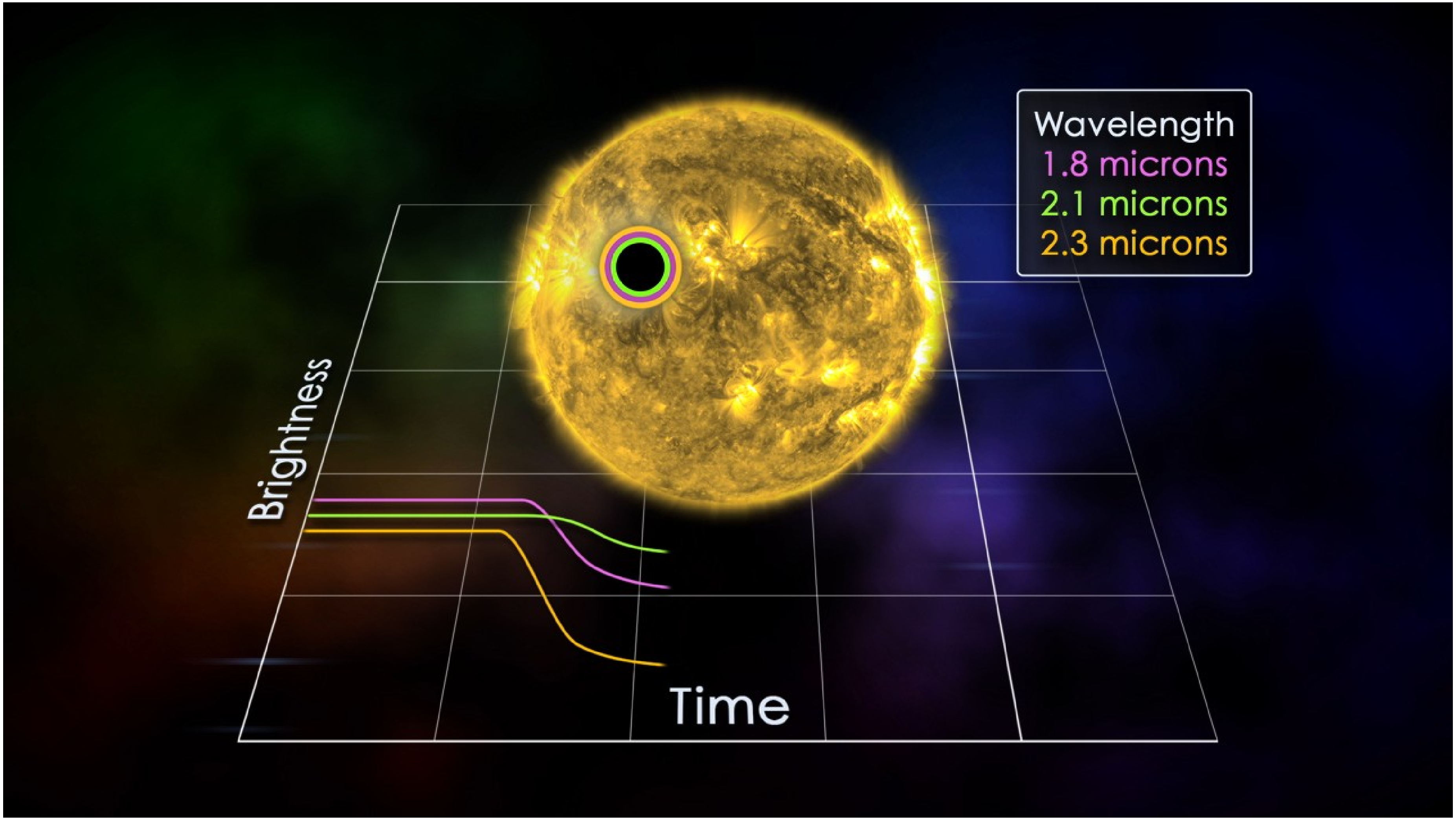

Planet atmospheres